Modelling wildfire in an intermediate complexity earth system climate model - exploring the importance of timestep and weather variability

Étienne Guertin

A Thesis
In the Department
of
Geography, Planning, Environment

Presented in Partial Fulfillment of the Requirements
For the Degree of Master of Science (Geography) at
Concordia University
Montréal, Québec, Canada

December 2017

CONCORDIA UNIVERSITY

School of Graduate Studies

This is to certify that the thesis prepared

By: Étienne Guertin

Entitled: Modelling wildfire in an intermediate complexity earth system climate model - exploring the importance of timestep and weather variability

and submitted in partial fulfilment of the requirements for the degree of

Master of Science (Geography, Urban and Environmental Studies)

complies with the regulations of the University and meets the accepted standards with respect to originality and quality.

Signed by the final Examining Committee:

_____ Chair

Dr. Norma Rantisi

_____ Internal examiner

Dr. Lawrence Mysak

_____ External examiner

Dr. David Huard

_____ Supervisor

Dr. H. Damon Matthews

Approved by:

_____

Dr. Norma Rantisi, Chair of Department

_____

Dr. André Roy, Dean of Faculty of Arts and Science

Date _____

ABSTRACT

Modelling wildfire in an intermediate complexity earth system climate model - exploring the importance of timestep and weather variability

Étienne Guertin

Fire is an integral part of the Earth system, interacting in complex ways with humans, vegetation and climate. Global fire activity is an important driver of the carbon cycle and could have important feedback effects on climate in a climate change context. Despite its potential importance, fire modelling as an integral part of global vegetation-climate models has only been developed in the past two decades, following the availability of global fire activity satellite products. This research aims to parameterize wildfire in an intermediate complexity earth system climate model coupled to a dynamic global vegetation model. I used a mechanistic fire model which simulates a burned area per grid cell based on a number of fires and the average burned area per fire. The fire parametrization was originally designed and calibrated for more realistic weather with more variability. Due to the simplicity of the atmosphere module of the climate model used, I explored the effect smaller modelling timesteps as well as prescribing natural variability to the simulated climatology. The simulations show no effect of timestep, while adding natural variability to the simulated climatology improves the global spatial correlation (R) of burnt fraction with observations. The best model (R=0,36; global burned area underestimated by 63%), however, does not capture the crucial difference of fire regime between the highly burning tropical savannas and the unburnt rainforests. This research shows the essential role of simulated weather variability rather than modelling timestep in generating realistic fire patterns in the context of this earth system climate model of intermediate complexity. Additional calibration could potentially improve the simulated fire and would allow the simulation of potential feedbacks within the fire-climate-vegetation system in a climate change context.

ACKNOWLEDGEMENTS

I would like to thank:

My supervisor Damon H. Matthews for his availability, his openness, his patience and his insights in this project.

Jean-Sébastien Landry for his invaluable help at guiding me through the literature of global fire modelling and providing me with advice at the beginning of the project.

Marc-Olivier Brault and Michael Eby for their help with the FORTRAN language and the UVic ESCM, and Donny Seto for his laugh and his help with technical issues.

Julie Lorrain, pour tes petites attentions et ton écoute qui ont fait toute une différence.

TABLE OF CONTENTS

LIST OF FIGURES

LIST OF TABLES

LIST OF ABBREVIATIONS

AVC: Above-ground vegetation carbon

BF: Burned fraction

ESCM : Earth System Climate Model

GBA: Global burned area

GCM: Global Circulation Model

GFED : Global Fire Emissions Database

GVC: Global above-ground vegetation carbon

UVic : University of Victoria

1. INTRODUCTION

Fire interacts with global vegetation distribution and structure, the carbon cycle, climate and human activities (Bowman *et al.*, 2009). Modelling has shown that without fire, global tree cover would reach two times its actual extent (27% vs. 56%; Bond, Woodward and Midgley, 2005) and savanna ecosystems could become closed canopy forests (Murphy and Bowman, 2012). Global fire-caused carbon emissions (i.e. gross carbon emissions to the atmosphere due to fire, including deforestation fires) amount today to about 20% of anthropogenic CO_2 emissions from fossil fuel burning and cement production (Yang *et al.*, 2015; van Der Werf *et al.*, 2010;). During the 20th century, between 20%-50% of fire-caused carbon emissions have not returned to the terrestrial carbon pool (Li, Bond-Lamberty and Levis, 2014; Yue *et al.*, 2014; Yang *et al.*, 2015). Fire is also an important driver of inter-annual atmospheric CO_2 growth anomaly (van der Werf, 2004) and significantly contributes to other greenhouse gas (van der Werf *et al.*, 2010; Ciais *et al.*, 2013) and aerosol (Andreae and Marlet, 2001) emissions. Regional and global fire activity projections do not agree to which extent climate and fire will interact in a climate change context (Westerling *et al.*, 2006; Williams *et al.*, 2009, Krawchuk *et al.*, 2009). Moreover, these studies of future fire activity do not treat fire as an integral part of the global climate-vegetation system. Despite being an integral part of the Earth system and a potentially important component of climate change, fire modelling is still a young science. In the last two decades, fire modelling has gradually been incorporated into global climate-vegetation models (eg. Arora and Boer, 2005; Thonicke *et al.*, 2010; Prentice *et al.*, 2011), following the availability of reliable global fire datasets (Giglio, Csiszar and Justice, 2006; Giglio, Randerson and Van Der Werf, 2013). To capture the dynamic interactions of fire with vegetation, human activity and climate, process-based approaches (i.e, that explicitly represent with varying levels of complexity the successive

steps that lead an ignition to biomass burning), rather than statistical approaches, are best suited to fire modelling. Modelling fire using this mechanistic approach is commonly done in a Dynamic Global Vegetation Model (DGVM) with prescribed climate data (e.g. (Li, Zeng and Levis, 2012)). To enable the climate feedback on fire in addition to the vegetation feedback, the DGVM can be coupled to an Earth System Climate Model (ESCM). Many fire models with varying levels of complexity and depth of coupling exist to this date, but it is not clear yet which level of complexity is required to accurately represent fire and its interactions with the Earth system (Hantson *et al.*, 2016). The process-based approach, combined with global fire products to calibrate the fire model parameters, has been successful at representing broad fire spatial patterns and seasonal variability (e.g. Li, Zeng and Levis, 2012, Li, Levis and Ward, 2013). However, these models forced climate data to drive the fire and vegetation component (Li, Zeng and Levis, 2012; Thonicke *et al.*, 2010) or used simulated climatology from Global Climate Models (GCMs) to drive future fire simulations (Pechony and Shindell, 2009; Knorr, Jiang and Arneth, 2015). The potential feedbacks between fire, vegetation and climate are thus currently not being assessed in the scientific literature. To achieve a reasonable fire activity that would enable reaching such goal, it is not clear yet which amount of variability is required by the simulated climatology and vegetation of an ESCM-DGVM.

1.1 Research goal

The scientific goal of the current thesis is to assess the signifiance of potential feebacks between fire, climate and vegetation in a climate change context. In order to reach this goal, I integrated a process-based fire model (Li, Zeng and Levis, 2012) to an intermediate complexity ESCM coupled to a DGVM and I evaluated the coupled model in terms of its ability to represent global fire activity. I addressed the shortcomings of the climatology of the

ESCM used by :

(1) adding natural variability to the simulated weather variables that drive the fire model;

(2) integrating the fire processes at an intermediate timestep, lying between the timestep at which the ESCM simulates variability and the one at which fire is modelled.

In the following sections, I will first review the emerging discipline of pyrogeography, that treats fire as an integral part of the human-Earth system (Bowman, O'Brien and Goldammer, 2013) by examining its human and climate change dimensions. I will then examine biome-specific fire ecology, review the global fire modelling efforts and discuss the improvements and challenges of this emerging discipline. I will follow with a description of the ESCM-DGVM I used, as well as the fire parameterization I chose to add. I will then present the methodology I used to add natural variability to the simulated weather variables and to simulate fire at different timesteps, followed by a sensitivity analysis of key parameters of the fire model inside this ESCM-DGVM. I will follow by presenting the results of the simulations and compare them to the ones obtained by the original parametrization and other similar fire parameterizations. I will finish by discussing the limitations of my approach, the next steps to take to improve the model and the potential feedbacks I hope to assess with a working fire model.

2. LITERATURE REVIEW

2.1 Pyrogeography

Wildfires are processes triggered by an ignition. If there is enough dry fuel at the ignition point, a fire then starts. The fire spreads depending on many factors including vegetation type, fuel dryness, temperature, human suppression and wind direction and speed (Krawchuk and Moritz, 2014).

2.1.1 Human dimension

During the preindustrial period (1000-1800 A.D.), the global fire regime was controlled by precipitation and during the industrialisation period, the main influence shifted to humans because of deforestation fires for agriculture (Pechony and Shindell, 2010). Humans now play a central role regarding fire and blur its natural interactions with climate (Bowman *et al.*, 2011, Bowman *et al.*, 2014). In developing economies, many forests are rapidly being converted to agricultural land and at the same time, migration to urban areas is increasing biomass accumulation in abandoned rural areas (Bowman *et al.*, 2013). Tropical forests in Asia and Amazonia, which are traditionally almost immune to fire, have become increasingly vulnerable due to the expansion of agricultural frontiers (Bowman *et al.*, 2013). In Indonesia, the 1997 El Niño extended dry season increased the extent of deforestation fires (Tacconi, 2003). In developed economies, fire-suppression effort is high in increasingly populated suburban areas at the interface with wildlands (Bowman *et al.*, 2009). Fire management policies have aimed at completely suppressing fires (Bowman *et al.*, 2013) to protect infrastructure, plantations, forest resources and agricultural land. However, this management practice has led to the accumulation of high fuel loads, increasing the risk of high-intensity wildfire which were not previously present in the ecosystem (e.g. Ponderosa pine in the

western United States; Bowman *et al.*, 2013). These high-intensity fires can kill entire stands of trees (Allen *et al.*, 2002; Syphard *et al.*, 2009). High levels of grazing can reduce fire frequency by allowing woody plants to grow and create a closed canopy where the flammable grass is outcompeted (Sankaran, Ratnam and Hanan, 2004; Werner, 2005). Effects of humans on fire also include an increased number of ignitions due to population growth, greater accessibility to remote areas and the spread of flammable plants (Bowman, O'Brien and Goldammer, 2013).

2.1.2 Climate change dimension

Fire-caused carbon emissions over the 1901-2010 period have been estimated to 2.43 petagrams of carbon per year (Pg C yr^{-1}) on average (Yang *et al.*, 2015). Comparatively, anthropogenic CO_2 emissions from fossil fuel burning and cement production were 7.6-9.0 Pg C yr^{-1} for the 2002-2011 period (Ciais *et al.*, 2013). Although burning biomass emits CO_2, the effect on the climate is not comparable to the effect of CO_2 emissions from fossil fuel burning, because of vegetation regrowth and decomposition and land surface albedo changes (Landry and Matthews, 2015). Modelling has shown that during the 20th century, the terrestrial carbon pool has lost 0.32-1.00 Pg C yr^{-1} due to fire-caused carbon emissions (Li, Bond-Lamberty and Levis, 2014; Yue *et al.*, 2014; Yang *et al.*, 2015). Global annual fire-caused carbon emissions were decreasing during the 20th century, but likely due to global climate change, the trend has reversed since the 1980's (Yang *et al.*, 2015) and fire frequency is predicted to increase during the 21st century (Pechony and Shindell, 2010; Daniau *et al.*, 2012; Moritz *et al.*, 2012; Ward *et al.*, 2012). Many regional studies have shown that large wildfire events have become more frequent since the end of the 20th century (Westerling *et al.*, 2006; Williams *et al.*, 2009). Yet, local increases of fire could be counter-balanced by

decreases at other locations, resulting in no net global change (Krawchuk *et al.*, 2009). There is currently no consensus, for more than half of the world's land area, on which direction fire activity will take in the next decades (Settele *et al.*, 2014), but there is less disagreement for longer-range predictions. Modelling groups generally agree that more fire will occur in the mid-to-high latitudes and less in the tropics by the end of this century (Moritz *et al.*, 2012). Fire could have a warming (Tosca, Randerson and Zender, 2013; Knorr, Jiang and Arneth, 2015) or cooling (Ward *et al.*, 2012; Landry, Matthews and Ramankutty, 2015) feedback on the climate that would have an important influence on contemporary climate projections (Bowman *et al.*, 2009; Flannigan *et al.*, 2009).

2.1.3 Fire ecology

-Tropical region

The highest level of fire activity is observed in tropical savannahs (Bowman, O'Brien and Goldammer, 2013; Pausas and Ribeiro, 2013). The rainfall pattern of these regions allows the accumulation of fuel loads during the intense wet season followed by drying to a high flammability point during the intense dry season. In tropical rainforests, where there is no dry season, the fuel loads are always high but the vegetation is never dry enough to allow fire. There, annual precipitation and net primary productivity (NPP; the net flux of carbon from the atmosphere to plants) are the highest. Rainfall and NPP are lowest in arid tropical regions, while they are intermediate in savannahs (Del Grosso, 2008). Although high fire activity is observed in most intermediate NPP regions, low fire activity is also observed. For example, in the tropics, large areas experiencing similar climatic conditions (i.e. strong wet-dry contrast between seasons) can either have an open canopy where high grass cover propagates fire and limits tree closure (tropical savanna) or a closed canopy where the absence of grass

inhibits fire (tropical seasonal forest). It has been hypothesized that these two biomes are stable states maintained by strong negative fire-tree cover feedbacks (grasslands in savannas encourage the spread of fire while trees in forests are more resistant to fire) and that whether the stability will be forest or grass dominated depends on the balance between the factors that influence tree growth rate and fire frequency (i.e. vegetation, climate, fire, atmospheric CO_2 and human factors). For example, increasing CO_2 concentrations likely explain the current trend of forest expansion in savanna ecosystems (Murphy and Bowman, 2012; Bowman *et al.*, 2014).

-Boreal region

Boreal forests have and will experience the most temperature rise of any forested region due to global warming (IPCC 2013). This will lead to more fire activity, which will increase CO_2 net emissions and reinforce the cycle by a positive feedback loop (Bond-Lamberty *et al.*, 2007). The largest wildfires are observed in sparsely populated areas (Archibald *et al.*, 2010) and the burned areas are on average 2.4 times larger for lightning caused fires than human caused fires for Canada. This suggests that without fire management in the boreal region, extreme wildfire events will be more frequent in a climate change context. Boreal wildfires are different across North American and Eurasian forests although the fire weather is similar. The North American fires are crown fires and thus more intense, while the Eurasian fires are less intense and consist of surface fires. This is due to the difference in dominant tree species – North American forests are dominated by trees that spread crown fires (fire embracers) while Eurasian trees suppress them (fire resisters). North American boreal forest fires should increase the spring albedo because of high fire mortality which will result in cooling while Eurasian boreal forests will probably be climate neutral or have a warming effect because surface fires cause less mortality and thus don't affect the albedo as

much. Current dynamic global vegetation models, by using a single needleleaf functional type, do not represent the contrasting fire strategies observed which are arguably as important for the global carbon and energy cycles as the savanna-tropical forests transitions (Rogers *et al.*, 2015).

2.2 Global fire modelling

Fire modelling, as any environmental modelling branch, is done with either statistical models or process-based models.

2.2.1 Statistical fire modelling

Statistical models derive empirical relationships between climate and fuel availability, and prescribe the probabilities of fire occurring (e.g. Moritz *et al.*, 2012 with fire counts). They are good at predicting fire regime in a modern day context given fuel and climate conditions. However, they are limited when it comes to predicting how fire regimes will change in an environment where, for example, climate, land use and vegetation distribution and structure become significantly different from their present day value or state. This is because these environmental variables then exceed the range of values or states on which the statistical model was built. In this expanded range, the complex interactions between climate, vegetation and fire often become non-linear. These interactions include, for example, the effect of atmospheric CO_2 on vegetation growth through water-use efficiency (Keenan *et al.*, 2016) and vegetation structure (Cramer *et al.*, 2001). This limitation of statistical models can be generalized to any environmental system that one tries to model, simply because the statistical models are dependent on the data they are based on and therefore on the state of the system at the time of collecting the data (Costanza and Ruth, 1998). Despite their inherent

weaknesses, statistical models are essential to inform process-based models of key variables, such as (Bistinas *et al.*, 2014) - Sec. 2.2.4.

2.2.2 Process-based fire modelling

Process-based fire models, on the other hand, are built from the series of mechanisms underlying biomass burning (e.g. from ignitions to burned area) and are integrated to DGVMs driven by climate data (e.g. Li, Zeng and Levis, 2012) or coupled to ESCMs. Both models carry varying degrees of complexity, allowing the representation of feedbacks on fire from vegetation (DGVM) or vegetation and climate (ESCM-DGVM) in a changing environment.

DGVMs model vegetation by representing a Plant Functional Types (PFT) (e.g. broadleaf trees, evergreens, bushes, C3 and C4 grasses). The PFTs compete with each other in every grid cell of the model according to, for example, a competition model (e.g. Lotka-Volterra competition model (Goel, Maitra and Montroll, 1971; implemented in Cox, 2001), for resources (e.g. light and water) inputted by prescribed weather data or data from an ESCM which is coupled to the DGVM.

Burned area is the most common output variable in fire modelling because it allows easy calculation of the burned biomass (burned area * biomass per unit area) which is needed to estimate greenhouse gases and aerosols emissions. It is also readily available in satellite observation data products (Giglio, Randerson and Van Der Werf, 2013). The authors of the fire models described in the current section used the Global Fire Emissions Database (GFED) burned area products version 3 (Giglio, Csiszar and Justice, 2006) and version 4 (Giglio, Randerson and Van Der Werf, 2013) to calibrate and evaluate their parameterizations.

Global fire regimes have long been neglected in climate models because of the lack of consistent global fire observations. Satellite monitoring in the past 20 years has provided the scientific community with homogeneous and global observations of fire regimes (e.g. Giglio, Randerson and Van Der Werf, 2013). These new data products, which give global burned area values, have made possible the study of global fire trends and their prediction. Many modelling groups have parameterized fire disturbance in vegetation using a mechanistic approach (i.e., a process based approach that represents the mechanism that leads to biomass burning) (Thonicke *et al.*, 2001; Venevsky *et al.*, 2002; Arora and Boer, 2005; Pechony and Shindell, 2009; Kloster *et al.*, 2010; Li, Zeng and Levis, 2012; Li, Levis and Ward, 2013).

A common process based approach to fire modelling has three main steps: (1) fire occurrence, (2) fire spread and (3) fire impacts. The fire occurrence step depends on ignition sources (natural and anthropogenic) and the characteristics of the vegetation and specifies the fire counts per grid cell. The fire spread step estimates the area burned by those fires depending on vegetation characteristics and weather conditions and in the last step, the resulting emissions and impacts on vegetation and the carbon cycle are estimated.

At first, ignition was considered ubiquitous and fire counts were solely a function of minimum fuel load (i.e. under a certain quantity of fuel, no fire can start) and maximum litter moisture thresholds (Thonicke *et al.*, 2001). Fire occurrence was then converted to burned area assuming a direct relationship between the proportion of a year where fire occurred and the fraction of that grid cell that would burn in the same period (Thonicke *et al.*, 2001). However, a grid cell that burned at least once a day for 365 days was assumed to totally burn, but the temporal and spatial aspects of fire are not exclusively dependent (Chuvieco, Giglio and Justice, 2008). Additionally, this method assumes that fire does not spread between grid cells. This early fire modelling attempt showed nonetheless fairly good agreement with

observations.

In a second study, the same lead authors improved their model by following more closely the three step approach previously described (Venevsky *et al.*, 2002). They added ignition probability as a function of lightning frequency, population density and socioeconomic status. They also used a fire danger index, the Nesterov Index (NI; originally developed for Siberian forests management) to determine if a fire would start (fire count) after an ignition occurred. The NI is calculated from daily temperature at 15:00 LT, dew point temperature and precipitation. It takes into account that fire danger increases for consecutive days until a threshold amount of precipitation occurs, in which case the index falls back to zero. The ignition triggers and the Nesterov index allowed the estimation of fire counts per grid cell. Burned area was then calculated for every fire counted as a function of the average fire spread rate and fire duration, which were assumed to be the same for every fire in a given cell on a given day. The major improvement of this model over the previous one is that burned area was explicitly described for fires.

Building on these previous studies, another research group developed a general process based approach for fire modelling (Arora and Boer 2005). Their parameterization was meant to be replicable in DGVMs coupled to climate models. They were the first to include lightning frequency explicitly as an ignition source. Fire occurrence depended on the availability of fuel to burn (minimum threshold biomass), its readiness to burn (maximum threshold soil moisture) and the probability of ignition (human and lightning). They added an elliptical function to describe how fire would spread. The shape and size of the burned area was determined by wind speed and direction, soil moisture and a constant fire spread rate. The major improvement they brought was that in every grid cell, daily burned area was the product of the fire occurrence probability for a 1000km2 area with the average burned area

per fire, divided by 1000km^2. However, this approach inherently limited the maximum number of fires to a single fire/day/1000km^2; it thus did not capture large burned areas in regions where there are more than 1 fire/day/1000km^2. The CO_2 emissions were then estimated according to the PFTs present in the burned area. The authors used weather observation records to drive the meteorology of the model and assessed how well it represented reality by comparing the burned area, CO_2 emissions and the fire return interval (FRI) to fire observation data. The FRI is the time interval between the burning of an area equivalent to the total area of a region. The model, driven by sub-daily climate data, performed well (global spatial correlation of burned area with observations R=0.52; Arora and Boer 2005). However, fire was underestimated in some regions where more than one fire/day/1000km2 occurred and did not account for anthropogenic effects on fire.

This parameterization of fire in DGVMs was further improved by taking into account human caused ignitions and human suppression of fires (as a function of population density) and land use change (prescribed from an external dataset) (Kloster *et al.*, 2010). The simulated burned area and emissions generally agreed with observations spatially (R = 0.53) except for two regions where over (South America) or under (Africa) estimation occurred. The authors attribute this local bias to the biomass estimation from the DGVM used. Also, including fire suppression greatly improved the spatial correlation between simulated and observed values (R = 0.33 without fire suppression).

Li, Zeng and Levis (2012) improved the parameterization by explicitly representing the number of fires occurring in every grid cell. The burned area was then the product of fire counts within the average fire spread area. This new parameterization eliminated the problem encountered by Arora and Boer (2005) regarding the underestimation of large burned areas when they were generated by many small fires. The authors also improved the fire spread and

biomass combustion parameterization by adding key elements to them. The new fire model showed further improved spatial correlation with observations (R=0.60). However, the authors pointed out areas that required improvement: anthropogenic impacts on fire were only dependent on population density, average fire duration was taken as one day (but fires are often multi day events) and vegetation dynamics processes were only updated annually. The same lead authors improved their parameterization by splitting fire in different categories (i.e. agricultural, deforestation, peat and non-peat) (Li, Levis and Ward, 2013). Agricultural fires were parameterized according to GDP and population density. Deforestation fires happened in the Amazon, and these were controlled by a prescribed deforestation rate and climate conditions. The coefficients used were derived from regressions maximizing the explained variance from the GFED3. Peat fires were also controlled by climate conditions. GDP was added to population density to explain fire occurrence. The authors simulated fire for the 1997-2004 period while driving the model with weather and socioeconomic observation records. The model simulated the fire regime and fire emissions from the four categories in good agreement with the GFED3 and better than Li, Zeng and Levis (2012) (R=0.69; Li, Levis and Ward, 2013).

Other fire models include one which takes into account the multiday nature of fire (Le Page *et al.*, 2015) and one which parameterizes wind speed so that it has a decreased influence on fire spread (and thus burned area) at high wind speeds, as suggested by comparison of modelled and observed burned area (Lasslop, Thonicke and Kloster, 2014).

Another fire parameterization combined the parameters described so far and predicted fire counts instead of burned area, outside a DGVM (i.e. with prescribed vegetation data) (Pechony and Shindell 2009; R=0.74). They used the Vapour Pressure Deficit (VPD) as an indicator of flammability conditions, a parameter calculated from temperature and relative

humidity. Additionally, their method required monthly precipitation and vegetation density. The higher agreement with observations in this case is not comparable to the others because it represents fire counts, not burned area and because the prescription of vegetation data removes the biases associated with its simulation. Burned area, as noted previously, is more desirable in a climate modelling context because it can be used to estimate biomass burning and then atmospheric emissions of CO_2 and other aerosols. However, this method, by its simplicity and its compatibility with a monthly time step, could be used to model the first part of wildfires, the fire counts.

2.2.4 Statistically-informed process-based models

The fire modelling studies previously presented have been criticized for their use of relationships that were not validated by statistical analysis of satellite observations. A simple multiple logistic regression analysis of burned area against vegetation, weather and anthropogenic predictor variables has challenged the assumed direct causation of some variables widely used in fire modelling (Bistinas *et al.*, 2014). They have found that emerging patterns (i.e. relationship observed between two variables when not controlling for any other variable) between burned area and some predictors were in fact explained by underlying relationships with other variables. For example, lightning frequency, which is widely used in fire modelling as a cause of ignition, varies in the same manner as the seasonally changing angle at which the solar radiation enters the atmosphere. After controlling for this seasonal solar variation, the lightning frequency did not have a significant effect on burned area. Bistinas *et al.* (2014) concluded that although lightning frequency most likely had an effect on the number of fires that start, it was not an important factor controlling monthly burned area in the end. Instead, fire spread and the presence of humans to suppress it could be more

important determinants of the burned area, as suggested by (Knorr *et al.*, 2014). This affirmation, although valid in the present day climatology, should be taken cautiously in the context of climate change, which will likely change the lightning frequency (Romps *et al.*, 2014). Another widely held assumption was that at low population densities, burned area increased with density but that at higher densities, population density had a suppression effect on fire; this was the emerging pattern observed when plotting population density against burned area (e.g. Knorr *et al.*, 2014). However, Bistinas *et al.* (2014) found that when taking into account NPP, and land use change (cropland and grazing-land areas), population density had a strong negative effect on burned area *even* at low densities. The authors explained the apparent positive relationship between burnt area and population density observed at low densities by the strong positive correlation between NPP and population at low densities (NPP is always low where population density is low and low NPP means low burned area). However, Bistinas *et al.* (2014) used a generalized linear model, which assumes linear relationships and they do not seem to have tested the relationship separately for low population densities only. The observed increase in burned area associated with an increase in population density, at low densities, could therefore still exist independently of NPP and the other controls used by Bistinas *et al.*, (2014), but this effect could not be captured in their multiple linear regression approach. In their analysis, the strongest predictors of monthly burned area were the number of dry days (+), the monthly maximum temperature (+), the net primary production (+), the ratio of actual to equilibrium evapotranspiration (-), the grass/shrub cover (+), cropland area (-), grazing-land area (+), population density (-) and the diurnal temperature range (+). Cropland areas fragment vegetation cover, limiting fire spread, and grazing-land areas increase burnt area probably because of an increase in flammable fine fuel (grass).

3. METHODS

3.1 Description of the UVic ESCM and its submodels

3.1.1 UVIC ESCM

The University of Victoria Earth System Climate Model (UVic-ESCM) (Weaver *et al.*, 2001) is an intermediate complexity model of 3.6° X 1.8° which contains a 19 layer ocean general circulation model coupled to a thermodynamic/dynamic sea-ice model, a single layer thermo-mechanical land ice model and a single layer reduced complexity vertically integrated energy-moisture balance atmospheric model. The atmospheric and sea-ice models are updated every 15 hours and the ocean every 30 hours. Every four ocean time steps, the atmosphere and sea-ice models, which have accomplished eight time steps by that time, are coupled to the ocean model. With the default settings, this coupling of all modules thus occurs every 5 model days. Present-day winds are prescribed in the atmosphere model and a dynamical wind feedback is added to allow a first order approximation of wind stress changes in a changing climate. Precipitation occurs when relative humidity reaches 85%. Simulated globally-averaged precipitation per year is in good agreement with observations, but at shorter time scales and spatially, it suffers from a lack of variability compared to reality.

3.1.2 TRIFFID

The Top-down Representation of Interactive Foliage and Flora Including Dynamics (TRIFFID) (Cox, 2001) is the DGVM coupled to the UVIC ESCM. TRIFFID explicitly models five plant functional types (PFT): broadleaf trees, needleleaf trees, C_3 grasses, C_4 grasses and shrubs. When coupled to an ESCM, climate variables influence vegetation structure, distribution and growth, which change land-surface parameters and affect atmospheric CO_2 concentration. The areal coverage, leaf area index and canopy height of

each PFT are calculated for each grid cell periodically (normally every ten days) based on carbon available in the land surface scheme and a Lotka-Volterra competition model. Carbon availability is derived from net carbon fluxes calculated every thirty minutes. Carbon fluxes are the difference between photosynthesis and plant respiration and depend both on climate and atmospheric CO_2 concentration. Carbon is transferred to the soil in the land surface scheme by litterfall. From the soil, carbon is transferred to the atmosphere by microbial respiration, which depends on soil moisture and temperature. TRIFFID explicitly describes vegetation in detail but it is less complex than other DGVMs in terms of PFT diversity. For example, the Community Land Model (CLM; Levis *et al.*, 2004) used in fire modeling by Li, Zeng and Levis (2012) and Kloster *et al.* (2010) has 10 PFTs instead of the 5 PFTs of TRIFFID in the UVic ESCM. Currently, fire is represented in TRIFFID as a constant loss rate attributed to disturbance independent of climate and vegetation.

3.1.3 MOSES

The UVic ESCM-TRIFFID is coupled to a land surface scheme (Meissner *et al.*, 2003). The land surface scheme is a simplified version of the Met Office Surface Exchange Scheme (MOSES). The scheme is a single layer which describes the land module in terms of lying snow, skin and soil temperature and soil moisture content. It recognizes the five PFTs of the TRIFFID as well as bare soil. Carbon and water fluxes to the atmosphere and runoff are calculated four times per day. Those fluxes are time-averaged and are passed to the ocean and atmosphere every five days and to the TRIFFID every month. The TRIFFID model then passes vegetation information to the land surface scheme which updates its vegetation-dependent parameters (every month). The simulated vegetation structure is spatially correlated with observations at r=0.635, which is comparable to TRIFFID coupled to atmospheric general circulation models. However, specific areas show low correlation due to

complex physiological responses not captured by global vegetation models and because of climate anomalies simulated by the UVic ESCM.

3.2 Fire parameterization

The fire parameterization used in this thesis models fire as a mechanistic process (see Fig. 21; adapted from Li, Zeng and Levis, 2012) with three mains steps: (1) fire occurrence, (2) fire spread and (3) fire impacts. Li, Zeng and Levis (2012) designed fire occurrence and fire spread for a daily (or less) timestep and fire impacts for a daily to annual timestep. I used the parametrization by Landry, Matthews and Ramankutty (2015) for fire impacts, designed for a 30 day timestep. I integrated all three steps at both a 5 and 30 day timesteps. The parameters used in the formulas of the following Section (3.2) are described in Table 1.

3.2.1 Fire occurrence

-Ignition sources

The number of ignitions N_i in a grid cell is

$$N_i = I_n + I_a \quad (1)$$

where I_n is the number of natural ignitions and I_a the number of anthropogenic ignitions. The number of natural ignitions is

$$I_n = I_l I_{ratio} \gamma \quad (2)$$

where I_l is the total number of lightning flashes, I_{ratio} is the ratio between the number of cloud-to-ground flashes and the number of lightning flashes and γ is the ignition efficiency of cloud-to-ground lightning (Latham and Schlieter, 1989). I_{ratio} is given by

$$I_{ratio} = \frac{1}{5.16 + 2.16\cos(3 * lat)} \quad (3)$$

where *lat* is the latitude in degrees (Prentice and Mackerras, 1977).

The number of anthropogenic ignitions I_a (count month^{-1}) is

$$I_a = 0.026452 * D^{0.4} \quad (4)$$

where D is the population density (number of people km^{-2}) (Li, Zeng and Levis, 2012).

-Fire counts

The fire counts N_f (*i.e.* the number of ignitions that start a fire) are

$$N_f = \begin{cases} 0 & snow > 0 \\ N_i * f_b * f_m * (1 - f_s) & snow = 0 \end{cases} \quad (5)$$

where *snow* is the amount of lying snow, f_b is the fuel availability, f_m is the fuel combustibility and f_s is the fire anthropogenic suppression (Li, Zeng and Levis, 2012). The three f functions vary between 0 and 1.

Fuel availability f_b is a function of biomass surface density and is given by

$$f_b = \begin{cases} 0 & B_{act} < B_{low} \\ \dfrac{B_{act} - B_{low}}{B_{up} - B_{low}} & B_{low} \le B_{act} \le B_{up} \\ 1 & B_{act} > B_{up} \end{cases} \quad (6)$$

where B_{act} is the actual biomass density (g C m^{-2}), B_{low} is the minimum biomass density at which a fire can start and B_{up} is the biomass density over which fuel availability no longer limits ignitions from starting fires (Li, Zeng and Levis, 2012).

Fuel combustibility f_m is

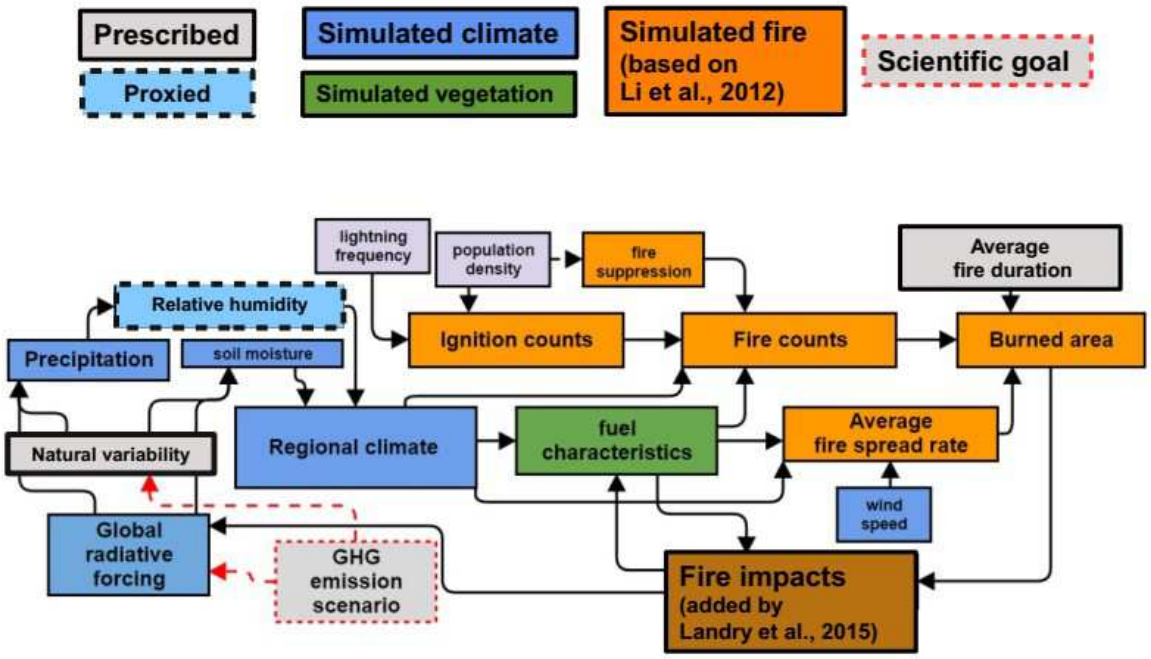

Figure 1: Fire parameterization diagram of the present study. Red dashes arrows represent a transient simulation using different GHG emission scenarios. The current study only looks at an equilibrium climate scenario.

$$f_m = f_{RH} * f_\theta \quad (7)$$

where f_{RH} is a function of relative humidity (RH) and f_θ is a function of soil moisture (Li, Zeng and Levis, 2012). Both functions vary between 0 and 1.

f_{RH} was given by

$$f_{RH} = \begin{cases} 1 & RH \le RH_{low} \\ \dfrac{RH_{high} - RH}{RH_{high} - RH_{low}} & RH_{low} < RH < RH_{high} \\ 0 & RH \ge RH_{high} \end{cases} \quad (8)$$

where RH_{low} is the RH below which ignitions are not limited by RH and RH_{high} is the maximum RH over which a fire cannot start.

f_θ is calculated from the soil moisture θ

$$f_\theta = \exp\left[-\pi\left(\frac{\theta}{\theta_e}\right)^2\right] \quad (9)$$

where θ is the soil moisture (sm) relative to that at saturation sm_{SAT} and θ_e is the extinction coefficient of soil wetness (Li, Zeng and Levis, 2012). The choice of θ_e determines a threshold soil moisture level at which the success of ignitions is very small.

Fire suppression f_s by humans is a function of population density D and is applied to fire counts by the following relationship:

$$f_s = \epsilon_1 - \epsilon_2 \exp(-\alpha D) \quad (10)$$

where ε_1 and ε_2 and α are constants (Li, Zeng and Levis, 2012; Pechony and Shindell 2009).

3.2.2 Fire spread

-Average fire duration

In Li, Zeng and Levis (2012), the average fire duration is assumed to be 1 day which is an underestimation of large scale wildfires which last many days in Li, Zeng and Levis (2012). This value is still a good estimate of fire duration, as it corresponds to the mathematical expectation of an empirically-derived exponential distribution of fire duration (Venevsky *et al.*, 2002).

-Average fire spread rate

Every fire counted spreads in an elliptical shape where the longest axis is in the downwind direction.

The length-to-breadth ratio L_B is estimated by

$$L_B = 1 + 10 * \left(1 - e^{-0.06\,w}\right) \quad (11)$$

where w is the wind speed in m s^{-1} (Arora and Boer 2005).

The head-to-back ratio H_B is given by

$$H_B = \frac{L_B + \left(L_B^2 - 1\right)^{1/2}}{L_B - \left(L_B^2 - 1\right)^{1/2}} \quad (12)$$

(Li, Zeng and Levis, 2012).

Fire spread rate in the downwind direction u_w ($m\ s^{-1}$) is

$$u_w = 2\,u_{max,i} * f_{RH} * f_{root} * g(w) \quad (13)$$

where $u_{max,i}$ is the maximum fire spread rate in natural vegetation regions for vegetation type i and f_{root} and $g(w)$ are functions of soil moisture and wind speed respectively and vary between 0 and 1 (Li, Zeng and Levis, 2012). f_{root} is a surrogate for vegetation moisture content (Arora and Boer, 2005). The 2 factor comes from the corrigendum of Li, Zeng and Levis (2012). In Li, Zeng and Levis (2012), f_{root} is dependent on the water content of the different soil layers associated with different vegetation types. Since the land surface scheme of the UVic is single layered (Meissner *et al.*, 2003), f_{root} will be constant among plant functional types.

f_{root} is given by

$$f_{root} = 1 - \tanh\left(\frac{1.75\,\beta_{root}}{\beta_e}\right)^2 \quad (14)$$

where β_{root} is the availability of water in the soil and β_e is an extinction wetness constant above which the probability of fire is negligible (Arora and Boer, 2005).

Fire parameter	Description	Value	Units	reference
γ	cloud-to-ground lightning ignition efficiency	0.25	dimensionless	Latham and Schlieter (1989)
θ_e	extinction coefficient of soil wetness	0,69 0,35 0,3	dimensionless	Li, Zeng and Levis (2012) Arora and Boer (2005) Thonicke et al. (2001)
sm_{SAT}	saturated soil moisture	458	kg m^{-2}	Li, Zeng and Levis (2012)
Θ_w	wilting soil moisture content	0,136	dimensionless	Arora and Boer (2005)
Θ_c	critical soil moisture content	0,242	dimensionless	Arora and Boer (2005)
$g(0)$	constant	0,05	dimensionless	Li, Zeng and Levis (2012)
B_{low}	minimum biomass density for fuel availability	155	g C m^{-2}	Li, Zeng and Levis (2012)
B_{up}	maximum biomass density for fuel availability	1050	g C m^{-2}	Li, Zeng and Levis (2012)
RH_{low}	minimum relative humidity for fuel combustibility	0,3	dimensionless	Li, Zeng and Levis (2012)
RH_{high}	maximum relative humidity for fuel combustibility	0,7	dimensionless	Li, Zeng and Levis (2012)
ε_1	fire suppression constant	0.99 0.95	dimensionless	Li, Zeng and Levis (2012) Pechony and Shindell (2009)
ε_2	fire suppression constant	0.98 0.90	dimensionless	Li, Zeng and Levis (2012) Pechony and Shindell (2009)
α	fire suppression constant	0.025 0.05	dimensionless	Li, Zeng and Levis (2012) Pechony and Shindell (2009)
u_{max}	maximum fire spread rate	0,11/0,15/0,17/0,2/0,2		Li, Zeng and Levis (2012)
Climate param.	**Description**	**Value**	**Units**	**reference**
pr_{min}	min. precipitation threshold (rh_{fire})	1E-07	mm s^{-1}	
pr_{max}	max. precipitation threshold (rh_{fire})	1E-05	mm s^{-1}	

Table 1: Fire and climate parameters values used. Broadleaf trees (BT), needleleaf trees (NT), shrubs (S), C3 grass (C3) and C4 grass (C4).

β_{root} is given by

$$\beta_{root} = \max\left[0, \min\left(1, \frac{\theta - \theta_w}{\theta_c - \theta_w}\right)\right] \quad (15)$$

where θ_w is the wilting soil moisture content (the volumetric soil moisture concentration below which stomata close) and θ_c is the critical soil moisture content (the volumetric soil moisture concentration above which stomata are not sensitive to soil water) (Arora and Boer, 2005).

g(w) is given by

$$g(w) = \frac{2L_B}{1+\frac{1}{H_B}} g(0) \quad (16)$$

(Li, Zeng and Levis, 2012), where g(0) is a constant.

The fire spread rate perpendicular to the wind u_p is

$$u_p = u_{max} * g(0) * f_{root} * f_{RH} \quad (17)$$

(Li, Zeng and Levis, 2012).

-Average burned area

The average burned area B_a (km^2) of a single fire is then defined according to the formula for the area of an ellipse, namely,

$$B_a = \frac{\Pi * u_w^2 * t^2}{(4L_B)} * \left(1+\frac{1}{H_B}\right)^2 * 10^{-6} \quad (18)$$

(Li, Zeng and Levis, 2012), where t is the average fire duration in seconds and 10^{-6} converts m^2 to km^2.

-Burned area

The burned area B_A (km^2) in the grid cell is then the product of the number of fires with the average burned area per fire,

$$B_A = N_f * B_a \quad (19)$$

3.2.3 Fire impacts

Once the burned fraction is calculated, it is then applied to the vegetation fraction for each PFT using the code from Landry, Matthews and Ramankutty (2015, Supplemental material).

It takes into account that woody PFTs will not burn completely because of islands of vegetation that remain unburned. This amounts to a 5% difference between modelled gross and net burned area. The agriculture fraction (crop + pasture) is prescribed in the UVic ESCM (see Fig. 3) and is not included in the vegetation fraction – fire therefore does not happen in the agriculture fraction.

3.3 Fire model integration in the UVic ESCM-TRIFFID

I created new variables to store the 5/30 days averages of simulated climate variables required in the fire model. Every fire step (5 or 30 days), the time averaged gridded precipitation calculated in the atmosphere module and the soil moisture in the land surface module are used in the fire module according to the fire parameterization (Sec. 3.2).

3.3.1 Description of prescribed data

I converted all the climatology data I prescribed to the fire model to a monthly timestep. I reduced the high resolution data sets listed in table 2 to the UVic ESCM resolution (1.8° x 3.6°) using a custom linear interpolation code. The code averages the values of the small cells contained inside each larger cell and splits the smaller cells that are part of two different large cells appropriately. For the 5 days fire model, the monthly lightning flash rate dataset was divided by 6 instead of using the 5 days average, which limits the variability compared but still gives a reliable estimate of the lightning climatology.

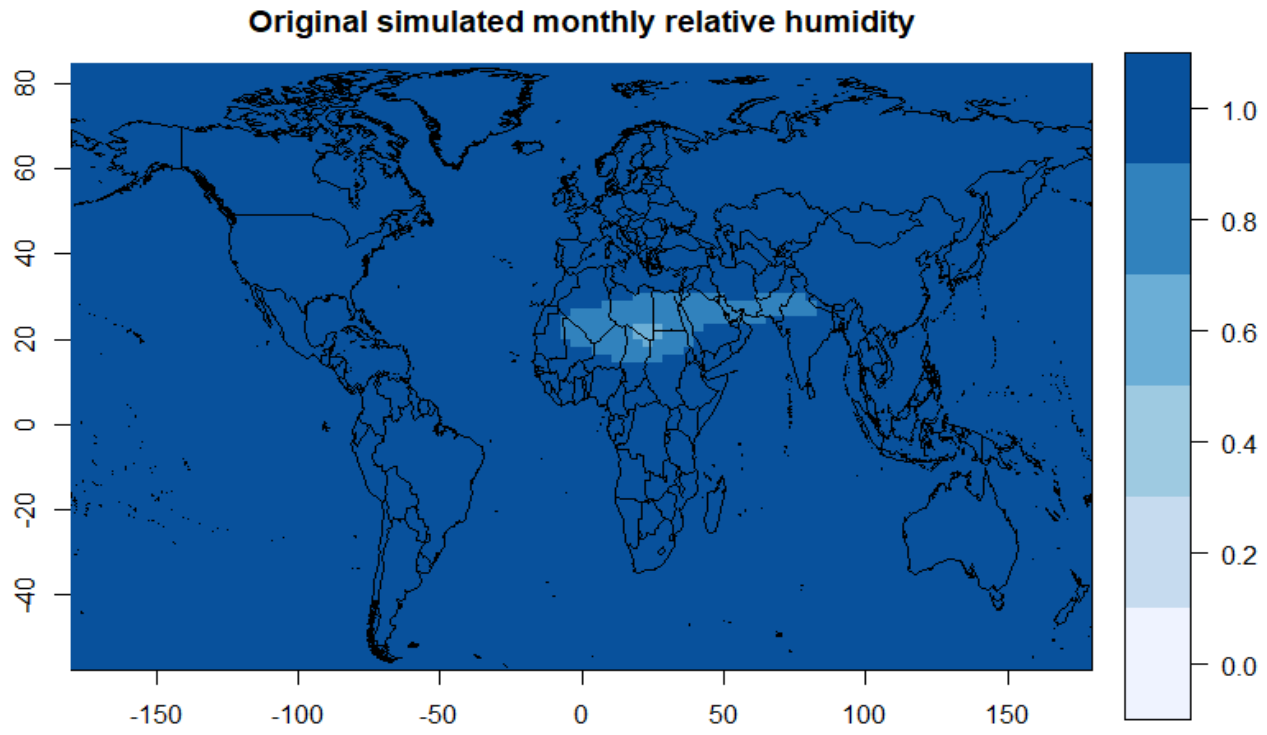

Figure 2: Monthly relative humidity simulated by the UVic ESCM. All months are the same except for minor changes in the drier area over the Sahara region.

3.3.2 Simulated climate variability

3.3.2.1 Relative humidity

Li, Zeng and Levis (2012) prescribed observation-based climate data to drive the CLM–DGVM, while I used the simulated climate variables outputted by the UVic ESCM. The two main climate variables used by the fire parametrization were relative humidity and soil moisture. Relative humidity is poorly simulated in the UVic ESCM, as shown by Fig. 2, and definitely lacked the necessary variability to have a meaningful effect on the simulated fire.

In order to address this shortcoming, I used the more variable simulated precipitation to derive a relative humidity field as follows:

$$rh_{fire} = \begin{cases} 0 & pr_{fire} \leq pr_{min} \\ \dfrac{pr_{fire} - pr_{min}}{pr_{max} - pr_{min}} & pr_{min} < pr_{fire} < pr_{max} \\ 1 & pr_{fire} \geq pr_{max} \end{cases} \quad (20)$$

where rh_{fire} is the relative humidity field used in the fire model, pr_{fire} is the simulated precipitation (with or without added prescribed variability), pr_{min} and pr_{max} are arbitrary precipitation value thresholds determining the null and saturated relative humidity. These two values (Table 1**),** when projected at a yearly timescale, correspond to a desert climate (pr_{min}) and a semi-arid climate (pr_{max}). They were chosen to optimize seasonal and spatial variability of the relative humidity field generated by the simulated climatology (Fig. A1, first column).

Variable	units	period*	source
		Prescribed	
Lightning rate	flashes km^2 $month^{-1}$	1995-2013	Cecil, Buechler and Blakeslee, 2014
Population density	people km^{-2}	2000	Jones and O'Neill 2016
Precipitation variability	mm $month^{-1}$	1901-2013	Schneider et al. 2014
Soil moisture variability	kg m^{-2}	1948-2016	Fan and van den Dool, 2004
Crop and pasture lands	fraction of gridcell	1800	UVic ESCM default
		Model validation	
Fire counts	number of fires km^{-2} $month^{-1}$	2001-2006	Giglio, Csiszar and Justice, 2006
Burned fraction	fraction of gridcell $month^{-1}$	2001-2012	Giglio, Randerson and Van Der Werf, 2013
Relative humidity	unitless	1948-2014	Kalnay et al. 1996
Soil moisture	kg m^{-2}	1948-2016	Fan and van den Dool, 2004

Table 2: Description of datasets used for forcing and validation.
*Time intervals are averaging periods.

3.3.2.2 Natural variability

Since the monthly and 5 days simulated soil moisture and relative humidity (rh_{fire}) had poor variability compared to reality (Fig. A1, first and last column), I added the standard deviation of observed precipitation and soil moisture products (Table 2) to the simulated values (Figs.

A1-A2, center column). A visual analysis of histograms for randomly selected gridcells from diverse biomes showed that both monthly-averaged precipitation and soil moisture were generally normally distributed across the observation periods (113 and 58 years, respectively). Every fire step (5 or 30 days), when variability was added, the precipitation and soil moisture used in the fire model in a grid cell were given by

$$pr_{fire} = pr_{\mathrm{sim}} + stdev_{pr} * rndnum \;\; ; \;\; pr_{fire} \geq 0 \quad (21)$$

$$sm_{fire} = sm_{\mathrm{sim}} + stdev_{sm} * rndnum \;\; ; \;\; sm_{fire} \geq 0 \quad (22)$$

where pr_{sim} and sm_{sim} are the simulated precipitation and soil moisture, *stdev* their respective monthly standard deviation and *rndnum* is a random normal number.

3.4 Study design

3.4.1 Model evaluation

I used the version 4 of the Global Fire Emissions Database (GFED4) (Giglio, Randerson and Van Der Werf, 2013) as a benchmark to evaluate the fire parameterizations. The dataset I used was created by Landry, Matthews and Ramankutty (2015). This dataset varies monthly from 2001-2010 at the UVic ESCM spatial resolution and restricts the burned fraction product to data from MODerate resolution Imaging Spectroradiometer (MODIS) only. The global burned area of GFED4 amounts to 350Mha yr^{-1}, 4Mha yr^{-1} of which corresponds to deforestation fires (based on van der Werf et al (2010)). GFED4 does not detect small fires that have been estimated to affect 120 Mha/yr, mostly (80%) from croplands, savannahs and grasslands (Randerson et al, 2012).

3.4.2 Multimodel comparison

Prior to creating a suite of models to compare against each other, I performed a sensitivity

analysis on relevant parameters, θ_e and B_{high}, to determine their effect on the fire simulation. Increasing B_{high}, the threshold at which fuel availability does not limit fire anymore, strongly decreased the spatial variability of the simulated burned area relative to GFED4, without improving the spatial correlation. Only θ_e improved the simulated burned area and was retained in the multimodel simulations. I also tested the effect of the added variability to precipitation and soil moisture, as well as the 5 days and 30 days timesteps (Table 3).

model name	θ_e	timestep (days)	prescribed variability
H5pv	0,69	5	precipitation
H5spv	0,69	5	precipitation and soil moisture
M5pv	0,6	5	precipitation
L5spv	0,55	5	precipitation and soil moisture
H5nov	0,69	5	none
H30spv	0,69	30	precipitation and soil moisture
H30nov	0,69	30	none
GFED4		30	

Table 3: Settings of the different equilibrium simulations. The soil moisture availability parameter θ_e was tested for high (H), medium (M) and low (L) values and variability (v) was added to soil moisture (s) and/or precipitation (p) or none (no).

3.4.3 Simulation settings

Each simulation ran for 300 years with constant forcings, at which time the models reached equilibrium in terms of global vegetation carbon. The atmospheric CO_2 concentration (282.2 ppm) and agricultural fraction (Fig. 3) were prescribed for year 1800 while population density and the benchmark fire regime were from the beginning of the 21st century (Table 2). This time period difference between these forcing datasets was unavoidable, and its impact on the results is examined in the discussion. To compare the models against each other, I used the monthly burned fraction (BF) and above-ground vegetation carbon (VC) and their yearly global values for the last 10 years of each simulation at equilibrium.

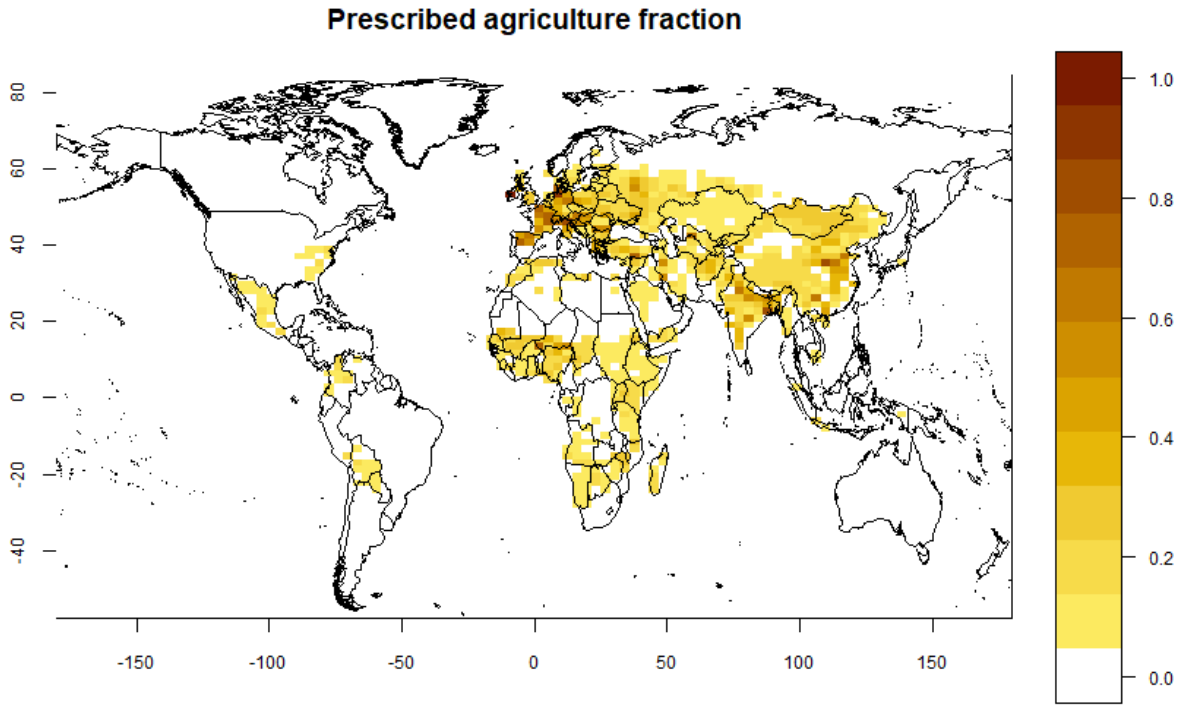

Figure 3: Constant agriculture fraction prescribed to the simulations (year 1800). Fire does not happen in the agriculture fraction of grid cells.

4. RESULTS

I used the GFED4 to evaluate the different fire models in terms of BF and VC. Fig. 4 and Fig. 5 show the spatial evaluation of the different models (Table 3) using Taylor Diagrams.

4.1 Taylor Diagrams

Taylor Diagrams are used to summarize how well patterns match each other breaking them down into three statistics (Taylor, 2001). These diagrams are especially useful when applied to complex models such as global climate models. A variable is assessed for different models versus its observed value in terms of global spatial correlation, standard deviation and root mean squared error. The global spatial correlation describes the spatial match between the simulated and observed variable. The standard deviation describes the total global variability of the variable and the root mean squared error describes the total global bias of the simulation relative to the observation.

4.2 Simulated climate variables

The simulated relative humidity and soil moisture both generally showed seasonal variability comparable in timing to observations, but with a smaller amplitude. Some regions in the simulation had major discrepancies with observations.

4.2.1 Relative humidity

The relative humidity derived from the simulated precipitation (Fig. A1) reproduces the wet/dry season variability observed in the tropics, but with less seasonal variability and some discrepancies. The Amazon Basin is wetter from January-April and gets drier in July but this pattern isn't as clear as for the observed data. Over tropical Africa, seasonal variability occurs

but the central rainforest part is often drier than the adjacent tropical area experiencing the wet season (e.g. July and October in Simulated vs. Observed). In reality, the boreal forest has a low relative humidity in July, and in the other seasons the air water content is higher because of lower temperatures which lower the saturation threshold. In the simulations, July is the only month with some relative humidity, because most rain precipitation, the proxy for relative humidity, happens in the summer at those latitudes. This pattern is particularly striking in the Eurasian boreal forest.

4.2.2 Soil moisture

Simulated soil moisture generally has a weaker seasonal variability than in reality (Fig. A2). Eastern continental USA is too dry in the UVic ESCM from April-October, while Western Continental North America should be drier all year-long. The Eurasian boreal forest is too wet in the eastern part. The observed tropical Africa's soil moisture is seasonally very variable, while the simulation shows poor variability. South America displays the same seasonal variability pattern as in the observations, but with less inter-seasonal variation.

4.3 Effect of timestep

The fire model timesteps (5 days or 30 days) produced the same BF or VC. For the simulations without added variability, the H30nov and H5nov had the same correlation coefficient, standard deviation and mean squared error (MSE) relative to the reference simulation using prescribed GFED4 burned area. The same happened for the simulations with added variability, with H30spv and H5spv which are juxtaposed in the three dimensional diagrams (Figs. 4 and 5).

4.4 Effect of natural climate variability

Adding natural variability to the precipitation used to generate the relative humidity field did not have a significant effect on the simulation either, as can be seen by comparing H5pv and H5nov. Adding variability to soil moisture, however, significantly improved the correlation coefficient of the burned fraction with GFED4 from R=0.28 (H5pv and H30nov) to R=0.36/0.37 (H5spv/H30spv; Table 4). The only benefit of not prescribing variability to soil moisture seems to be in the Amazon. There the burned fraction is lower for M5pv compared to L5spv despite that the increase in θ_e from L5spv to M5pv should increase burned fraction, signalling the stronger effect of adding soil moisture variability.

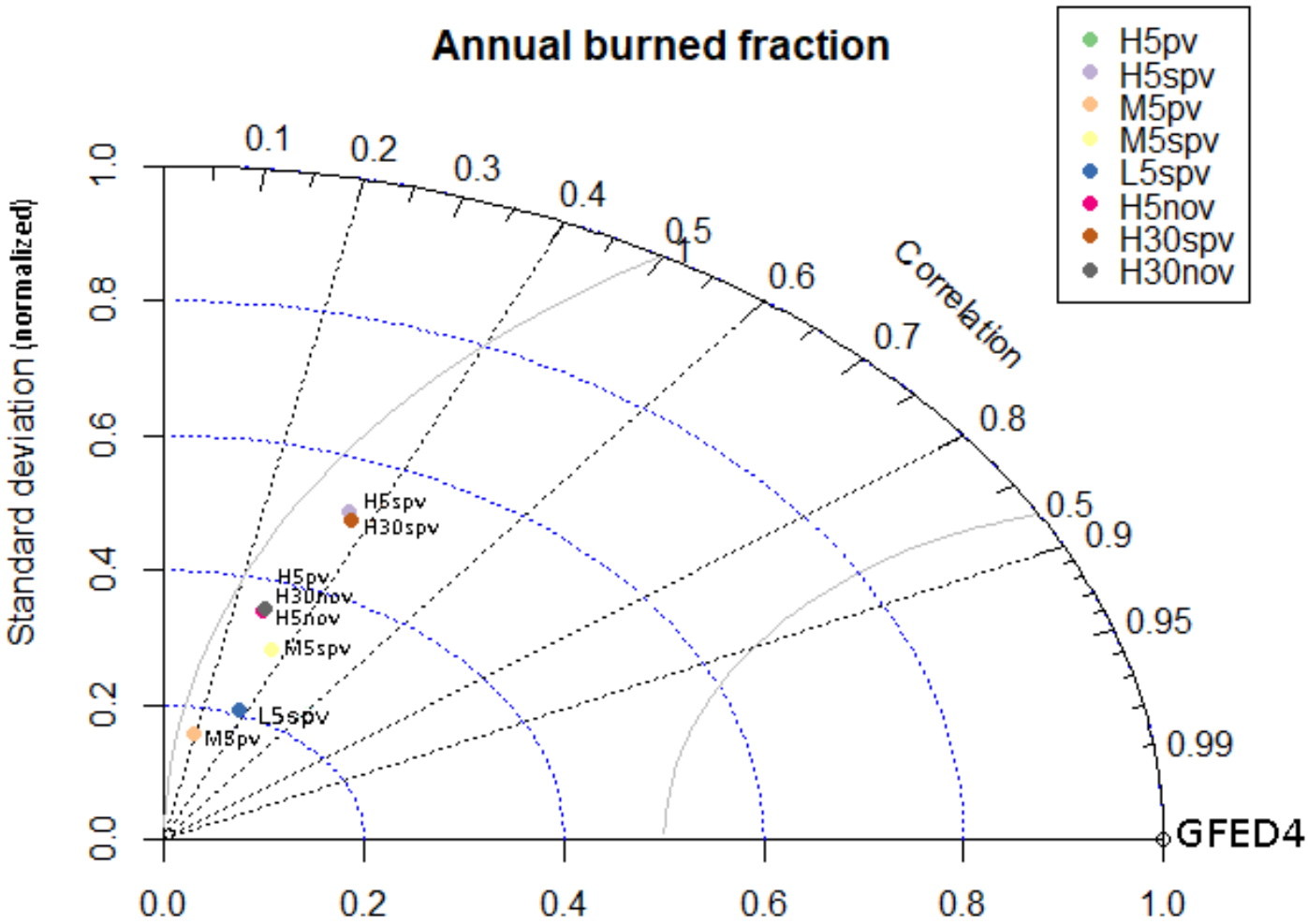

Figure 4: Taylor diagram of the simulated annual burned fraction for the different models. Description of models is given in Table 3. The black dashed lines represent the correlation coefficient intervals, the blue dashed curves the normalized standard deviation relative to the reference model using prescribed GFED4 fire regime and the gray curves represent the Mean Squared Error relative to GFED4.

4.5 Effect of θ_e

Increasing the value of the extinction coefficient of soil wetness, θ_e, increased the spatial variability of the simulated burned fraction, as shown by L5spv (low θ_e), M5spv (medium θ_e) and H5spv (high θ_e) in Fig. 4, and decreased the spatial variability of the above-ground vegetation carbon (Fig. 5). The global burned area (GBA) and global vegetation carbon (GVC) were affected similarly, with GBA increasing by more than 3x and GVC decreasing by 2.5x between L5spv and H5spv (Table 4).

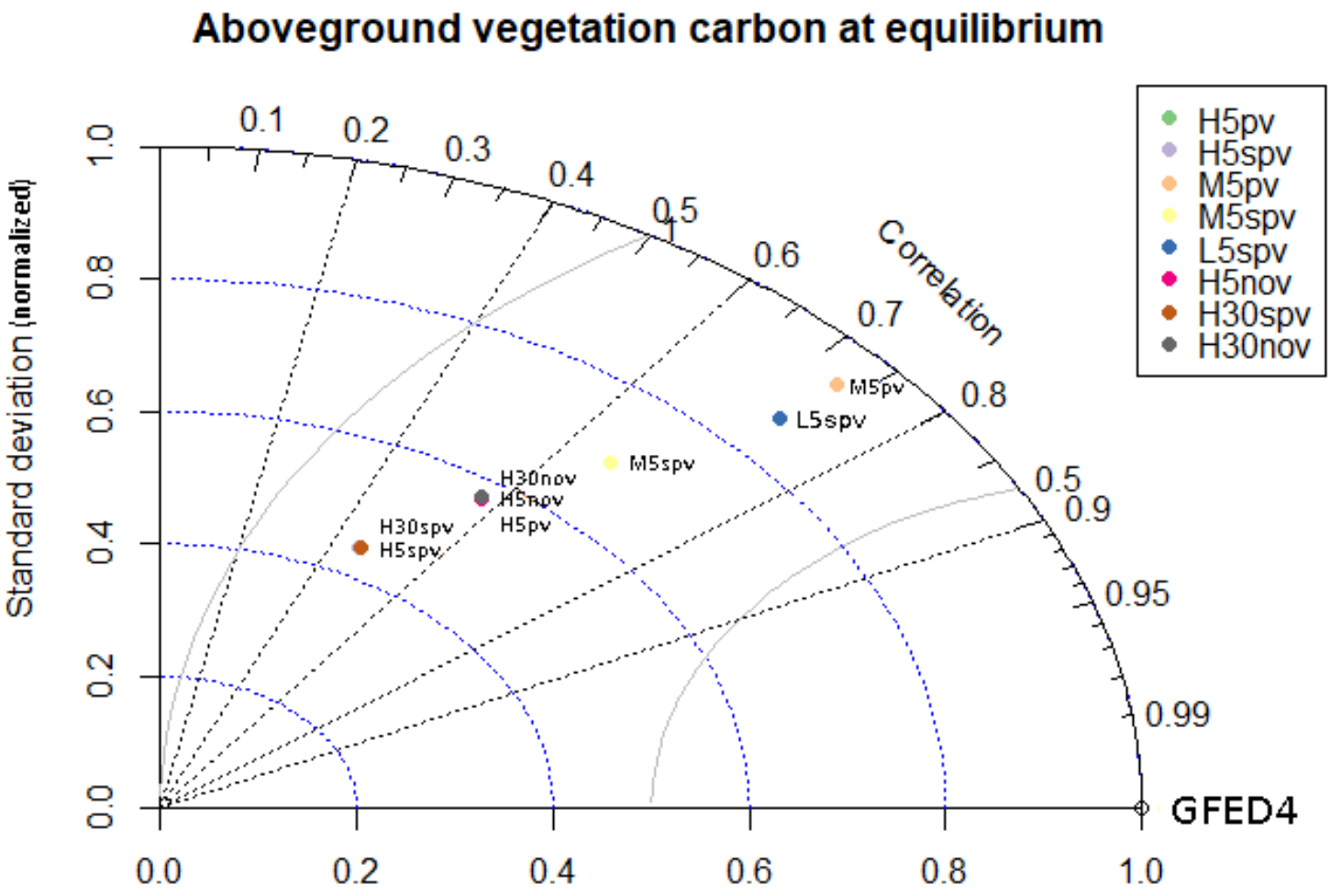

Figure 5: Taylor diagram of the simulated aboveground vegetation carbon for the different models. The description of models is given in Table 3. The black dashed lines represent the correlation coefficient intervals, the blue dashed curves the normalized standard deviation relative to the reference model using prescribed GFED4 fire regime and the gray curves represent the Mean Squared Error relative to GFED4.

4.6 Model evaluation

The two models that were the closest to GFED4 were H5spv/H30spv and L5spv. Given the effect of θ_e on burned fraction and aboveground vegetation carbon (Sec. 4.3), it is not a surprise to see in Table 4 that H5spv/H30spv produced the best combination of spatial correlation (R=0.36) and GBA (overestimated by 12-14%), at the cost of having the lowest spatial correlation for AVC (R=0.46 vs. 0.57-0.73 for other models) and global vegetation carbon (GVC; underestimated by 67%). On the other hand, L5spv produced both the highest spatial correlation for BF and AVC and underestimated GVC by 18% but GBA by 63% (Table 4). L5spv also simulated a low spatial variability for burned area (0.21 vs. 0.51 for H5spv/H30spv; Fig. 4). When looking at the spatially explicit annual burned fraction (Fig. 5), we see that H5spv/H30spv (shown as H30spv) overestimates burned fraction everywhere except in tropical Africa and northern Australia, while L5spv is more in agreement with GFED4 except for those two regions.

model	GBA (Mha yr^{-1})	GVC (Pg-C)	R (Burned fraction)	R (Vegetation carbon)
H5pv	**252**	**200**	**0,28**	**0,57**
H5spv	384	148	0,36	0,46
M5pv	**99**	**416**	**0,18**	**0,73**
L5spv	**124**	**366**	**0,36**	**0,73**
H5nov	260	204	0,28	0,57
H30spv	**372**	**149**	**0,37**	**0,46**
H30nov	259	207	0,28	0,57
GFED4	334	447	1	1

Table 4: Annual global burned area (GBA) and global vegetation carbon (GVC) simulated and their spatial correlation coefficient (R) with the GFED4 prescribed burned area simulation. Models in **bold** are examined more in depth.

Both models strongly overestimate burned fraction over the three main rainforests (Amazon, central Africa and Indonesia). This overestimation is stronger for H30spv, which results in the absence of vegetation in these areas at equilibrium (Fig. A4). In the L5spv simulation, the Amazon and Indonesia are correctly preserved but with a lower AVC; however the African vegetation is completely burned in the rainforest area that GFED4 preserves. The visual agreement between L5spv and GFED4 in terms of vegetation is also better for the Eurasian boreal forest and western USA, which are almost completely burned at equilibrium in H30spv (Fig. A4). Despite underestimating GBA by two thirds, L5spv is still better at predicting burned fraction because it preserves more accurately the large rainforest carbon pools than H5spv/H30spv. The global spatial correlation (R=0.36) is comparable to older and less complex fire parameterizations such as Glob-FIRM (R=0.39; Thonicke *et al.*, 2011) and the one used by Levis *et al.* (2004) (R=0.44). The GBA obtained, 124 Mha yr^{-1}, is also similar to these two fire modules (Glob-FIRM : 54 Mha yr^{-1}; Levis *et al.* (2004): 93 Mha yr^{-1}). However, the authors who designed the current fire parametrization (Li, Zeng and Levis, 2012) obtained a stronger global spatial correlation (R=0.60) and a GBA close to GFED3 (330 Mha yr^{-1} vs. 380 Mha yr^{-1} GFED3).

5. DISCUSSION

The results point to improvements that are necessary in order to be able to address the potential feedbacks between climate, vegetation and fire in a climate change scenario context.

5.1 Timestep and added natural variability

The absence of notable differences between simulating fire at a 5 or 30 days interval was expected when no natural variability was added to the simulated climate variables, given that the UVic ESCM simulates climate with very low variability at the 5 days timestep. The precipitation and soil moisture 5 and 30 days spatial time averages were in fact negligibly different even before adding variability. Adding variability to precipitation did not change its effect on burned fraction, probably because the relative humidity function (Eq. 8) that was affected by this did not vary much more with the added variability. There was no difference between 5 days and 30 days when I prescribed to soil moisture its natural variability. This result has, in fact, a simple mathematical explanation. The simulated 5 days and 30 days averages were the same for soil moisture, and I used the monthly standard deviation for both timesteps. The range of possible values was therefore identical regardless of the timestep, and the long term averages used to evaluate the models – 10 years in this case – converged to the same value. The 5 days standard deviation, if calculated, would have been larger than for 30 days because the extreme values in the observation dataset are less masked by time averaging as the time resolution increases.

I tested the effect of the monthly 2x standard deviation to emulate the 5 days standard deviation, and it increased the global burned area compared to the 1x standard deviation. However, I did not include this simulation in the Taylor Diagrams at the time of producing them. I assume 2x standard deviation would further increase the global spatial correlation of

burned fraction as well as the spatial standard deviation relative to GFED4.

The other possible effect of a 5 days timestep was to progressively reduce the burnable area by reducing the vegetation fraction in each gridcell over each 30 days interval, since vegetation regrowth happens every 30 days in the model while fire impacts happen at the fire timestep. The fire parameterization was designed to update vegetation according to burned area yearly (Li, Zeng and Levis, 2012). In areas with high fire activity, this method overestimates burned area because, over a one year period, the model potentially reburns the already burnt area multiple times. This overestimation is of concern for areas with high seasonal burned fraction, such as African savannas. In my simulations, however, the results do not show a significant difference in monthly burned area between the two timesteps. This is probably because the maximum simulated 5 days burned fraction (at most ~2% of grid cell per 5 days) was too small to significantly impact the remaining burning 5-days steps before regrowth. The absence of differences between 5 days and 30 days timesteps highlights the importance of climate variability rather than timestep for fire modelling in the context of an ESCM of intermediate complexity. In other words, timestep, in the present study, only matters because the climate variability appropriate to fire is intrinsic to shorter timesteps.

5.2 Comparison with Li, Zeng and Levis (2012)

The fact that Li, Zeng and Levis (2012) (Li *et al.* for the rest of this section) obtained significantly better results than my parametrization (Sec. 4.5) in key areas is probably largely due to the use of sub-daily climate data to drive their DGVM and simulating the burned fraction consequently at an hourly timestep. They captured the high burned fractions of tropical savannas and the null fraction in the African and Amazon rainforests (Li *et al.*; Fig. 8 – Mod-new), while my parametrization simulated a mostly homogeneous medium fraction

over those biomes (Fig. A3, L5spv), which leads to the disappearance of rain forests (Fig. A4 -L5spv). Both models capture the medium fraction in Northern Eurasia, although a visual comparison confirms that Li *et al.* obtain a better spatial correlation. My model better captures the spatial pattern of fire in North America, while Li *et al.* strongly overestimate fire in Continental North America. This is due to the fact that agricultural fractions are treated the same as vegetation fractions by Li *et al.*, while they are ignored in my parameterization. Their results thus lead to the overestimation of fire because crop PFTs burn easily in a natural context, while I underestimate fire in gridcells with high agricultural fractions. Both models do not capture the high burned fraction in Northern Australia. In my case, the TRIFFID underestimates vegetation density at this location (Fig. A5 vs. Fig A6) and therefore probably regrowth rate, which limits the possibility of an annual high burned fraction, although the simulated climatology's low variability probably does not capture the necessary fire weather in the first place (Figs. A3 and A4). The most important differences between the results of Li *et al.* and this study are the ability in the UVic ESCM to capture (1) the null burned fraction in tropical rainforests of Africa and the Amazon and (2) high burned fractions (>50%) in African savannas. These differences are important given that observations indicate that global burned area is largely controlled by African vegetation (66%; 1997-2004; van der Werf *et al.*, 2006).

5.3 Limitations due to relative humidity

One of the most notable limitations of the UVic ESCM for this project was the absence of spatial variability for the simulated relative humidity (Fig. 2), which is a key variable in the original fire parameterization (Li, Zeng and Levis, 2012). The use of precipitation as a proxy strongly improved the spatial variability of relative humidity and its seasonal pattern

(Fig. A1). The African rainforest (the area that is unburned in central Africa in GFED4, Fig. A3) has a relative humidity close to or at 100% all year long according to observations, while the simulated values tended to be lower than the surrounding tropical savannas in their respective wet season (Fig. A1). This difference contributed to the strong overestimation of burned fraction in this area, and the associated strong decrease of global vegetation carbon, due to the high carbon density of rainforests. Natural ignitions are abundant in tropical rainforests, especially in Africa (Fig. A9), but constantly high fuel wetness prevents fires from starting (Del Grosso, 2008). The fire counts were highly overestimated by the simulations (Fig. A8 vs. A7) probably because of relative humidity. Both fire counts and burned area depend on relative humidity through f_{RH} (Eq. 7 and 13, respectively), which means that burned area (fire counts * fire spread) is dependent on the square of f_{RH}. This directs us toward the parameter RH_{high} (Eq. 8), the relative humidity threshold value at which the air is too wet for ignitions to become fires. It was left unchanged from its original value (0.7) during the sensitivity tests, but lowering Rh_{high} could perhaps reduce the burning of the central African rainforest. In addition to being less variable than observations the simulated relative humidity was also lower on average. This lack of variability was exposed by the null effect of adding its natural variability to the simulated precipitation used as a proxy for relative humidity (Table 4). Narrowing and lowering the RH_{ow}-RH_{high} range might also increase the variability generated by Eq. 8 and improvement the spatial correlation (similar to that of θ_E) when adding the natural variability.

5.4 Agricultural land and vegetation

Central Asia, the Middle East, Southern South America and South Australia experience fire

activity in GFED4, but not in the UVic ESCM (Fig. A3). In the case of Southern South America and South Australia, part of the reason is that TRIFFID simulates vegetation in these areas with an underestimation bias (Fig. A6 vs. Fig. A5). The other major cause is that a large fraction (at least 0.5) of the land in these regions - and other regions - is cropland or pasture land (Figs. 3and7). The current fire model underestimates burned fraction in these areas by ignoring agricultural land, which represents 8-11% of global annual fire counts (2001-2003; Korontzi *et al.*, 2006) and about 4.7% of global burned area (Van Der Werf *et al.*, 2010) or 10% when including small fires (Randerson *et al.*, 2012). However, this overestimation is blurred by the

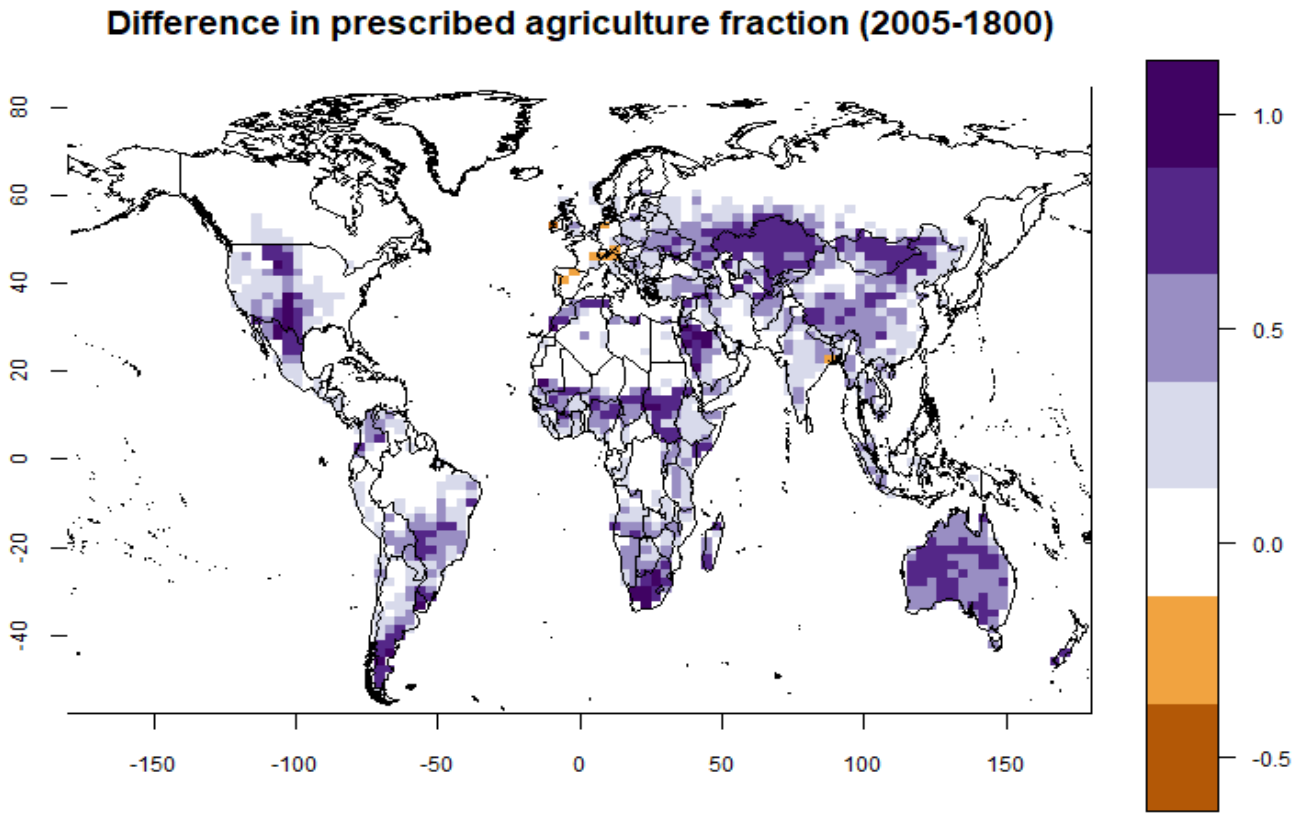

Figure 6: Difference between the agriculture fraction matching the time period (2005) of the burned fraction benchmark dataset (GFED4) and the burned fraction prescribed to the simulations (year 1800). The prescribed agricultural fraction period should have been 2005. Fire does not happen in the agriculture fraction of grid cells.

difference in the time period of the agricultural fraction prescribed (1800) and the burned fraction product used to evaluate the fire model (GFED4, 2001-2010). This difference in agricultural fraction likely caused an overestimation of burned area in most areas due to a smaller agricultural fraction (Fig. 7) (and thus a larger vegetation fraction). The areas most affected by this overestimation were South-Western USA and Mexico, South Africa, Northern Hemisphere African savannah and Southern Australia (Fig. A3**,** L5spv). The parameterization of agricultural fires in Li, Levis and Ward (2013) (along with peat fires and deforestation) improved the global spatial correlation of the model with GFED3 from R=0.6 to R=0.69. Adding this parameterization to the current fire model would correct the low biases of burned fraction for areas with high agricultural fraction and no vegetation. The net effect is not clear for areas with both high vegetation and agricultural fractions, as burning natural vegetation would be replaced with burning crops.

5.5 Other sources of uncertainty or bias

I identified minor sources of uncertainty or bias that should be taken into consideration when interpreting the results of my research, although the major simulation bias remains that the rainforests burned fraction is rather high.

-Limitations of the GFED

Although the current generation of GFED products are state of the art fire datasets, they do no detect small fires (less than 1km^2). These fires account for an additionnal 35% of global burned area (464Mha yr^{-1} vs. 345Mha yr^{-1}, Randerson *et al.*, 2012). They are particularly common in savannas (30.5 Mha yr^{-1}, +34%), woody savannas (46.4 Mha yr^{-1}, +27%), grasslands (9.6 Mha yr^{-1}, +24%) and croplands (11.8 Mha yr^{-1}, +123%). This means that all fire models are calibrated to capture a biased representation of global fire regime.

-GFED4 vs. GFED3

GFED4 (Giglio, Randerson and Van Der Werf, 2013) covers all land while GFED3 (Giglio, Csiszar and Justice, 2006) did not, and the dataproducts are calculated differently. These differences added to the different time periods decreased global burned area from 380 Mha yr^{-1} (GFED3, 1997-2004) to 350 Mha yr^{-1} (GFED4, 2001-2012). The current fire model was calibrated on GFED3 but its implementation in the UVic ESCM was evaluated using the GFED4. The largest discrepancy between both datasets is that GFED4 estimates the total burned area in North Hemisphere South America and Central America to be about 35% and 25% higher than GFED3 respectively (Giglio, Randerson and Van Der Werf, 2013).

-Root zone soil moisture function

The root zone soil moisture function β_{root} is PFT dependent (Li, Zeng and Levis, 2012; Arora and Boer, 2005) and depends on the soil water potential of each soil layer ((Levis *et al.*, 2004; Oleson *et al.*, 2010). I reduced it to a single value per grid cell in the UViC ESCM-TRIFFID, because this model has a single 1m deep soil layer (Meissner *et al.*, 2003). This could cause part of the high bias of burned fraction in rainforests, since rainforest trees can access water below 1m during drier periods (Stahl *et al.*, 2013).

-Relative humidity patterns

Another particularity of the relative humidity generated by the precipitation proxy was observed in the Northern Hemisphere boreal forests across North America and Eurasia. There, the relative humidity seasonal pattern was inversed (July was the wettest month in the simulations but the driest in observations, Fig. A1), because the precipitation proxy does not consider the influence of surface air temperature on relative humidity (Eccel, 2012).

However, this didn't seem to affect the fire model because of the presence of snow (Eq. 5) and the absence of ignitions in the winter months (Fig. A9), that could otherwise potentially burn due to low observed relative humidity (Fig. A4).

5.5 Deforestation fires

Deforestation fires are not distinguished from non deforestation fires in GFED3, the dataset used to calibrate the current fire parametrization (Li, Zeng and Levis, 2012) (except for θ_e). This means that areas prone to deforestation fires were modelled as non-deforestation fire areas in the present study. Although deforestation fires represent a small fraction of GBA (2.8% - the 1997-2004 average; Li, Bond-Lamberty and Levis, 2014), they have a significantly higher emission to burned area ratio. They account for about 20% of annual global fire CO_2 emissions (van der Werf *et al.*, 2010, Li, Levis and Ward, 2013) and about 50% of fire emissions that do not return to vegetation through regrowth (van der Werf *et al.*, 2010). It is therefore important to parameterize these fires, as done by Li, Levis and Ward (2013), in the hope of improving the accuracy of the simulated carbon cycle.

6. CONCLUSIONS

The major findings of this research project are that weather variability is a key driver of fire regimes and that the timestep in modelling only matters because of the intrinsic variability of simulated variables at a short time scale.

The scientific goal of this thesis was to assess the potential feedbacks between climate, vegetation and fire in a climate change context. In order to reach that goal, I parameterized fire in the intermediate complexity UVic ESCM-TRIFFID using a process based approach developped by Li, Zeng and Levis (2012). This fire parameterization – or similar parameterizations on which it is based – was designed and used in many other ESCM-DGVMs with a higher degree of complexity (Thonicke *et al.*, 2001; Venevsky *et al.*, 2002; Arora and Boer 2005; Kloster *et al.*, 2010; Li, Zeng and Levis, 2012; Li, Levis and Ward, 2013). All models simulated the burnt area at a daily or sub-daily timestep and at a finer spatial resolution than the UVic ESCM, with climate data taken from GCMs or observations prescribed to the terrestrial components. Their land and vegetation modules were able to represent more PFTs and multiple soil layers interacting with the water use of PFTs. These differences can all potentially explain the deficiencies of the fire model coupled in this thesis.

The main shortcoming of the UVic ESCM was probably the lack of variability and possible bias in the simulated climatology, necessary to reproduce the appropriate fire weather. I addressed this by integrating the fire module at a finer timestep than the interval at which variability was captured by the UVic ESCM (5 days instead of 30 days) and by adding natural variability to the simulated climate variables of interest for the fire model. The timestep did not directly affect the representation of fire – instead it was the natural variability attached to the timestep that increased the global spatial correlation of burned fraction with observations.

The best parameterization obtained (R=0.37; GBA = 124Mha yr^{-1}) performed similarly to previous less complex parameterizations by Thonicke *et al.* (2011) (Glob-FIRM : R=0.39; 54Mha yr^{-1}) and Levis *et al.* (2004) (CTEM-FIRE: R=0.44; 93Mha yr^{-1}), although its original implementation in the CLM-DGVM by Li, Zeng and Levis (2012) fared significantly better (R=0.60; GBA is underestimated by 13% vs. 63% for this thesis). However, unlike any of these three models, the present parameterization did not capture at all the large difference of annual burned fraction between the rainforests and savannas of the Amazon and Africa, which causes rainforests to burn down completely in Africa and partially in the Amazon (Fig. A4). This discrepancy is potentially due to a biased relative humidity, which was proxied by the simulated precipitation field (Eq. 20). More generally, it is the lack of intrinsic variability in the model's climatology that causes its poor performance. Other minor problems include the biased agricultural fraction used (Figs. 3 and 7), and improvements could be made by formally parameterizing fires coming from deforestation and agriculture (Li, Levis and Ward, 2013).

The long term objective of integrating fire in an ESCM-DGVM of intermediate complexity is to represent and assess the importance of the many feedbacks of the fire-vegetation-climate system (Fig. 21), namely the feedbacks of fire on climate, sometimes mediated by vegetation. One of these feedbacks could happen in a climate change context through changes in vegetation composition in tropical savannahs. For example, it is likely that grass dominated African savannahs will transition to woody species dominated forests through CO_2 fertilization and increased precipitation (Murphy and Bowman, 2012). Climate projections generally agree that precipitation would increase in African tropical savannahs (Christensen, 2007), which would favor woody species over grassy species in the TRIFFID. Additionally

the maximal fire spread rate constant in the current fire model allows grassy vegetation (C3 and C4) to burn over an area close to 4x more than deciduous trees. This transition would have a negative effect on fire activity in this area and a positive effect on vegetation carbon accumulation, leading to a negative feedback on atmospheric CO_2 concentration.

Biomass burning increases land surface albedo, which has been shown to have a non-negligible regional cooling effect in increasingly burning boreal forests (Randerson *et al.*, 2006; Beck *et al.*, 2011) and globally with modelling (Landry and Matthews, 2015).

Fuel availability could eventually limit fire in areas where weather becomes drier, leading to a complete biome and fire regime switch. This fire regime change has been shown by modelling (Landry, Matthews and Ramankutty, 2015).

A possible positive feedback loop of fire on climate would happen at a regional scale through changes in evapotranspiration. A regional change in fire activity caused by climate-mediated change of precipitation would lead to a change of local evapotranspiration due to changing vegetation composition and density. This would in all cases lead to a positive feedback loop reinforcing the precipitation change. It is not clear, however, if this effect can be captured by the current climate-vegetation.

Assessing these potential feedbacks requires a reasonable representation of the broad spatial and temporal patterns of fire in terms of burned fraction, which is used to estimate fire emissions (Andreae and Merlet, 2001). A fire impacts module including pyrogenic emissions of aerosols and other greenhouse gases was already integrated in the UVic ESCM-TRIFFID by Landry, Matthews and Ramankutty, (2015).

In order to improve sufficiently this fire model, a careful tuning of the relative humidity field proxied by the simulated precipitation, as well as a careful sensitivity analysis of the relative importance of the different functions relating fire to climate and vegetation are necessary.

REFERENCES

Allen, C. D., Savage, M., Falk, D. A., Suckling, K. F., Swtnam, T. W., Schulke, T., Stacey, P. B., Morgan, P., Hoffman, M. and Klingel, J. T. (2002) 'Ecological Restoration of Southwestern Ponderosa Pine Ecosystems : a Broad Perspective', *Ecological Applications*, 12(5), pp. 1418–1433.

Andreae, M. O. and Marlet, P. (2001) 'Emission of trace gases and aerosols from biomass burning', *Global Biogeochemical Cycles,* 15(4), pp. 955–966. doi: 10.1029/2000GB001382.

Archibald, S., Scholes, R. J., Roy, D. P., Roberts, G. and Boschetti, L. (2010) 'Southern African fire regimes as revealed by remote sensing', *International Journal of Wildland Fire*, 19(7), pp. 861–878. doi: 10.1071/WF10008.

Arora, V. K. and Boer, G. J. (2005) 'Fire as an interactive component of dynamic vegetation models', *Journal of Geophysical Research*, 110(G2), pp. 1–20. doi: 10.1029/2005JG000042.

Beck, P. S. A., Goetz, S. J., Mack, M. C., Alexander, H. D., Jin, Y., Randerson, J. T. and Loranty, M. M. (2011) 'The impacts and implications of an intensifying fire regime on Alaskan boreal forest composition and albedo', *Global Change Biology*, 17(9), pp. 2853–2866. doi: 10.1111/j.1365-2486.2011.02412.x.

Bistinas, I., Harrison, S. P., Prentice, I. C. and Pereira, J. M. C. (2014) 'Causal relationships versus emergent patterns in the global controls of fire frequency', *Biogeosciences*, 11(18), pp. 5087–5101. doi: 10.5194/bg-11-5087-2014.

Bond-Lamberty, B., Peckham, S. D., Ahl, D. E. and Gower, S. T. (2007) 'Fire as the dominant driver of central Canadian boreal forest carbon balance', *Nature*, 450(7166), pp. 89–92. doi: Doi 10.1038/Nature06272.

Bond, W. J., Woodward, F. I. and Midgley, G. F. (2005) 'The global distribution of ecosystems in a world without fire', *New Phytologist*, 165(2), pp. 525–538. doi: 10.1111/j.1469-8137.2004.01252.x.

Bowman, D. M. J. S., Balch, J., Artaxo, P., Bond, W. J., Cochrane, M. A., D'Antonio, C. M., Defries, R., Johnston, F. H., Keeley, J. E., Krawchuk, M. A., Kull, C. A., Mack, M., Moritz, M. A., Pyne, S., Roos, C. I., Scott, A. C., Sodhi, N. S. and Swetnam, T. W. (2011) 'The human dimension of fire regimes on Earth', *Journal of Biogeography*, pp. 2223–2236. doi: 10.1111/j.1365-2699.2011.02595.x.

Bowman, D. M. J. S., Balch, J. K., Artaxo, P., Bond, W. J., Carlson, J. M., Cochrane, M. a, D'Antonio, C. M., Defries, R. S., Doyle, J. C., Harrison, S. P., Johnston, F. H., Keeley, J. E., Krawchuk, M. a, Kull, C. a, Marston, J. B., Moritz, M. a, Prentice, I. C., Roos, C. I., Scott, A. C., Swetnam, T. W., van der Werf, G. R. and Pyne, S. J. (2009) 'Fire in the Earth system.', *Science (New York, N.Y.)*, 324(5926), pp. 481–484. doi: 10.1126/science.1163886.

Bowman, D. M. J. S., Murphy, B. P., Boer, M. M., Bradstock, R. a, Cary, G. J., Cochrane, M. a, Fensham, R. J., Krawchuk, M. a, Price, O. F. and Williams, R. J. (2013) 'Forest fire management, climate change, and the risk of catastrophic carbon losses', *Frontiers in Ecology and the Environment*, 11(2), pp. 66–68.

Bowman, D. M. J. S., Murphy, B. P., Williamson, G. J. and Cochrane, M. A. (2014) 'Pyrogeographic models, feedbacks and the future of global fire regimes', *Global Ecology and Biogeography*, 23, pp. 821–824. doi: 10.1111/geb.12180.

Bowman, D. M. J. S., O'Brien, J. A. and Goldammer, J. G. (2013) 'Pyrogeography and the Global Quest for Sustainable Fire Management', *Annual Review of Environment and Resources*, 38(1), pp. 57–80. doi: 10.1146/annurev-environ-082212-134049.

Christensen, J. H. (2007) 'Regional Climate Projections', *Climate Change: The Physical Science Basis*, 27(2007), pp. 847–940. doi: 10.1080/07341510601092191.

Chuvieco, E., Giglio, L. and Justice, C. (2008) 'Global characterization of fire activity: Toward defining fire regimes from Earth observation data', *Global Change Biology*, 14(7), pp. 1488–1502. doi: 10.1111/j.1365-2486.2008.01585.x.

Ciais, P., Sabine, C., Bala, G., Bopp, L., Brovkin, V., Canadell, J., Chhabra, A., DeFries, R., Galloway, J., Heimann, M., Jones, C., Quéré, C. Le, Myneni, R. B., Piao, S. and Thornton, P. (2013) 'Carbon and Other Biogeochemical Cycles', *Climate Change 2013: The Physical Science Basis. Contribution of Working Group I to the Fifth Assessment Report of the Intergovernmental Panel on Climate Change*, pp. 465–570. doi: 10.1017/CBO9781107415324.015.

Costanza, R. and Ruth, M. (1998) 'Using dynamic modeling to scope environmental problems and build consensus', *Environmental Management*. Springer-Verlag, pp. 183–195. doi: 10.1007/s002679900095.

Cox, P. (2001) 'Description of the TRIFFID dynamic global vegetation model', *Hadley Centre, United Kingdom Meteorological Office*, (Technical Note 24), pp. 1–16. Available at: http://www.metoffice.gov.uk/media/pdf/9/h/HCTN_24.pdf (Accessed: 20 November 2015).

Cramer, W., Bondeau, A., Woodward, F. I., Prentice, I. C., Betts, R. A., Brovkin, V., Cox, P. M., Fisher, V., Foley, J. A., Friend, A. D., Kucharik, C., Lomas, M. R., Ramankutty, N., Sitch, S., Smith, B., White, A. and Young-Molling, C. (2001) 'Global response of terrestrial ecosystem structure and function to CO_2 and climate change: results from six dynamic global vegetation models', *Global Change Biology*. Blackwell Science Ltd, 7(4), pp. 357–373. doi: 10.1046/j.1365-2486.2001.00383.x.

Daniau, A.-L., Bartlein, P. J., Harrison, S. P., Prentice, I. C., Brewer, S., Friedlingstein, P., Harrison-Prentice, T. I., Inoue, J., Izumi, K., Marlon, J. R., Mooney, S., Power, M. J., Stevenson, J., Tinner, W., Andrič, M., Atanassova, J., Behling, H., Black, M., Blarquez, O.,

Brown, K. J., Carcaillet, C., Colhoun, E. A., Colombaroli, D., Davis, B. A. S., D'Costa, D., Dodson, J., Dupont, L., Eshetu, Z., Gavin, D. G., Genries, A., Haberle, S., Hallett, D. J., Hope, G., Horn, S. P., Kassa, T. G., Katamura, F., Kennedy, L. M., Kershaw, P., Krivonogov, S., Long, C., Magri, D., Marinova, E., McKenzie, G. M., Moreno, P. I., Moss, P., Neumann, F. H., Norström, E., Paitre, C., Rius, D., Roberts, N., Robinson, G. S., Sasaki, N., Scott, L., Takahara, H., Terwilliger, V., Thevenon, F., Turner, R., Valsecchi, V. G., Vannière, B., Walsh, M., Williams, N. and Zhang, Y. (2012) 'Predictability of biomass burning in response to climate changes', *Global Biogeochemical Cycles*, 26, p. GB4007. doi: 10.1029/2011GB004249.

Eccel, E. (2012) 'Estimating air humidity from temperature and precipitation measures for modelling applications', *Meteorological Applications*, 19(1), pp. 118–128. doi: 10.1002/met.258.

Fan, Y. and van den Dool, H. (2004) 'Climate Prediction Center global monthly soil moisture data set at 0.5° resolution for 1948 to present', *Journal of Geophysical Research*, 109(D10), p. D10102. doi: 10.1029/2003JD004345.

Flannigan, M. D., Krawchuk, M. A., De Groot, W. J., Wotton, B. M. and Gowman, L. M. (2009) 'Implications of changing climate for global wildland fire', *International Journal of Wildland Fire*, 18(5), pp. 483–507. doi: 10.1071/WF08187.

Giglio, L., Csiszar, I. and Justice, C. O. (2006) 'Global distribution and seasonality of active fires as observed with the Terra and Aqua Moderate Resolution Imaging Spectroradiometer (MODIS) sensors', *Journal of Geophysical Research: Biogeosciences*, 111(2), pp. 1–12. doi: 10.1029/2005JG000142.

Giglio, L., Randerson, J. T. and Van Der Werf, G. R. (2013) 'Analysis of daily, monthly, and annual burned area using the fourth-generation global fire emissions database (GFED4)', *Journal of Geophysical Research: Biogeosciences*, 118(1), pp. 317–328. doi: 10.1002/jgrg.20042.

Goel, N. S., Maitra, S. C. and Montroll, E. W. (1971) 'On the volterra and other nonlinear models of interacting populations', *Reviews of Modern Physics*, 43(2), pp. 231–276. doi: 10.1103/RevModPhys.43.231.

Del Grosso, S. (2008) 'Global potential net primary production predicted from vegetation class, precipitation, and temperature (vol 89, pg 2117, 2008)', *Ecology*, 89(10), p. 2971. doi: 10.2307/25661124.

Hantson, S., Arneth, A., Harrison, S. P., Kelley, D. I., Colin Prentice, I., Rabin, S. S., Archibald, S., Mouillot, F., Arnold, S. R., Artaxo, P., Bachelet, D., Ciais, P., Forrest, M., Friedlingstein, P., Hickler, T., Kaplan, J. O., Kloster, S., Knorr, W., Lasslop, G., Li, F., Mangeon, S., Melton, J. R., Meyn, A., Sitch, S., Spessa, A., Van Der Werf, G. R., Voulgarakis, A. and Yue, C. (2016) 'The status and challenge of global fire modelling',

Biogeosciences, 13(11), pp. 3359–3375. doi: 10.5194/bg-13-3359-2016.

IPCC. Summary for Policymakers. In: Climate Change 2013: The Physical Science Basis. Contribution of Working Group I to the Fifth Assessment Report of the Intergovernmental Panel on Climate Change. IPCC 1–29 (2013).

Jones, B. and O'Neill, B. C. (2016) 'Spatially explicit global population scenarios consistent with the Shared Socioeconomic Pathways', *Environmental Research Letters*. IOP Publishing, 11(8), p. 84003. doi: 10.1088/1748-9326/11/8/084003.

Kalnay, E., Kanamitsu, M., Kistler, R., Collins, W., Deaven, D., Gandin, L., Iredell, M., Saha, S., White, G., Woollen, J., Zhu, Y., Chelliah, M., Ebisuzaki, W., Higgins, W., Janowiak, J., Mo, K. C., Ropelewski, C., Wang, J., Leetmaa, a., Reynolds, R., Jenne, R. and Joseph, D. (1996) 'The NCEP/NCAR 40-year reanalysis project', *Bulletin of the American Meteorological Society*, pp. 437–471. doi: 10.1175/1520-0477(1996)077<0437:TNYRP>2.0.CO;2.

Keenan, T. F., Prentice, I. C., Canadell, J. G., Williams, C., Wang, H., Raupach, M. R. and Collatz, G. J. (2016) 'Recent pause in the growth rate of atmospheric CO2 due to enhanced terrestrial carbon uptake', *Nature Communications*. doi: 10.1038/ncomms13428.

Kloster, S., Mahowald, N. M., Randerson, J. T., Thornton, P. E., Hoffman, F. M., Levis, S., Lawrence, P. J., Feddema, J. J., Oleson, K. W. and Lawrence, D. M. (2010) 'Fire dynamics during the 20th century simulated by the Community Land Model', *Biogeosciences*, 7(6), pp. 1877–1902. doi: 10.5194/bg-7-1877-2010.

Knorr, W., Jiang, L. and Arneth, A. (2015) 'Climate, CO2, and demographic impacts on global wildfire emissions', *Biogeosciences Discussions*, 12(17), pp. 15011–15050. doi: 10.5194/bgd-12-15011-2015.

Knorr, W., Kaminski, T., Arneth, A. and Weber, U. (2014) 'Impact of human population density on fire frequency at the global scale', *Biogeosciences*, 11, pp. 1085–1102. doi: 10.5194/bg-11-1085-2014.

Korontzi, S., McCarty, J., Loboda, T., Kumar, S. and Justice, C. (2006) 'Global distribution of agricultural fires in croplands from 3 years of Moderate Resolution Imaging Spectroradiometer (MODIS) data', *Global Biogeochemical Cycles*, 20(2), p. n/a-n/a. doi: 10.1029/2005GB002529.

Krawchuk, M. a. and Moritz, M. a. (2014) 'Burning issues: statistical analyses of global fire data to inform assessments of environmental change', *Environmetrics*, 25(6), pp. 472–481. doi: 10.1002/env.2287.

Krawchuk, M. A., Moritz, M. A., Parisien, M.-A., Van Dorn, J. and Hayhoe, K. (2009) 'Global Pyrogeography: the Current and Future Distribution of Wildfire', *PLoS ONE*, 4(4), p. e5102. doi: 10.1371/journal.pone.0005102.

Landry, J.-S. and Matthews, H. D. (2015) ‘Fire versus fossil fuels: All CO2 emissions are not created equal.’, *Biogeosciences Discussions*, pp. 15185–15222. doi: 10.5194/bgd-12-15185-2015.

Landry, J.-S., Matthews, H. D. and Ramankutty, N. (2015) ‘A global assessment of the carbon cycle and temperature responses to major changes in future fire regime’, *Climatic Change*, pp. 179–192. doi: 10.1007/s10584-015-1461-8.

Lasslop, G., Thonicke, K. and Kloster, S. (2014) ‘SPITFIRE within the MPI Earth system model: Model development and evaluation’, *Journal of Advances in Modeling Earth Systems*, 6, pp. 740–755. doi: 10.1002/2013MS000284.Received.

Latham, D. and Schlieter, J. (1989) ‘Ignition probabilities of wildland fuels based on simulated lightning discharges’, *United States Department of Agriculture, Forest Service*, (Research Paper INT-411), p. 16. Available at: http://www.firemodels.org/downloads/behaveplus/publications/Latham_and_Schlieter_INT-411_1989_ocr.pdf.

Levis, S., Bonan, G. B., Vertenstein, M. and Oleson, K. W. (2004) *The Community Land Model’s Dynamic Global Vegetation Model (CLM-DGVM): Technical Description and User’s Guide*, *NCAR/Tn-459+Ia*. doi: 10.5065/D6P26W36 CN - 03559 LA - en.

Li, F., Bond-Lamberty, B. and Levis, S. (2014) ‘Quantifying the role of fire in the Earth system – Part 2: Impact on the net carbon balance of global terrestrial ecosystems for the 20th century’, *Biogeosciences*, 11(5), pp. 1345–1360. doi: 10.5194/bg-11-1345-2014.

Li, F., Levis, S. and Ward, D. S. (2013) ‘Quantifying the role of fire in the Earth system – Part 1: Improved global fire modeling in the Community Earth System Model (CESM1)’, *Biogeosciences*, 10(4), pp. 2293–2314. doi: 10.5194/bg-10-2293-2013.

Li, F., Zeng, X. D. and Levis, S. (2012a) ‘A process-based fire parameterization of intermediate complexity in a dynamic global vegetation model’, *Biogeosciences*, 9(7), pp. 2761–2780. doi: 10.5194/bg-9-2761-2012.

Li, F., Zeng, X. D. and Levis, S. (2012b) ‘Corrigendum to: A process-based fire parameterization of intermediate complexity in a dynamic global vegetation model’, *Biogeosciences*, 9(7), pp. 2761–2780. doi: 10.5194/bg-9-2761-2012.

Meissner, K. J., Weaver, A. J., Matthews, H. D. and Cox, P. M. (2003) ‘The role of land surface dynamics in glacial inception: A study with the UVic Earth System Model’, *Climate Dynamics*, 21(7–8), pp. 515–537. doi: 10.1007/s00382-003-0352-2.

Moritz, M. a., Parisien, M.-A., Batllori, E., Krawchuk, M. a., Van Dorn, J., Ganz, D. J. and Hayhoe, K. (2012) ‘Climate change and disruptions to global fire activity’, *Ecosphere*, 3(6), p. art49. doi: 10.1890/ES11-00345.1.

Murphy, B. P. and Bowman, D. M. J. S. (2012) ‘What controls the distribution of tropical forest and savanna?’, *Ecology Letters*, 15(7), pp. 748–758. doi: 10.1111/j.1461-0248.2012.01771.x.

Oleson, W., Lawrence, M., Bonan, B., Flanner, G., Kluzek, E., Lawrence, J., Levis, S., Swenson, C., Thornton, E., Dai, A., Decker, M., Dickinson, R., Feddema, J., Heald, L., Hoffman, F., Lamarque, J.-F., Mahowald, N., Niu, G.-Y., Qian, T., Randerson, J., Running, S., Sakaguchi, K., Slater, A., Stockli, R., Wang, A., Yang, Z.-L., Zeng, X. and Zeng, X. (2010) ‘Technical Description of version 4.0 of the Community Land Model (CLM)’. doi: 10.5065/D6FB50WZ.

Le Page, Y., Morton, D., Bond-Lamberty, B., Pereira, J. M. C. and Hurtt, G. (2015) ‘HESFIRE: a global fire model to explore the role of anthropogenic and weather drivers’, *Biogeosciences*, 12(3), pp. 887–903. doi: 10.5194/bg-12-887-2015.

Pausas, J. G. and Ribeiro, E. (2013) ‘The global fire-productivity relationship’, *Global Ecology and Biogeography*, 22(6), pp. 728–736. doi: 10.1111/geb.12043.

Pechony, O. and Shindell, D. T. (2009) ‘Fire parameterization on a global scale’, *Journal of Geophysical Research: Atmospheres*, 114(June), pp. 1–10. doi: 10.1029/2009JD011927.

Pechony, O. and Shindell, D. T. (2010) ‘Driving forces of global wildfires over the past millennium and the forthcoming century’, *Proceedings of the National Academy of Sciences*, 107(45), pp. 19167–19170. doi: 10.1073/pnas.1003669107.

Prentice, I. C., Kelley, D. I., Foster, P. N., Friedlingstein, P., Harrison, S. P. and Bartlein, P. J. (2011) ‘Modeling fire and the terrestrial carbon balance’, *Global Biogeochemical Cycles*, 25(July), pp. 1–13. doi: 10.1029/2010GB003906.

Prentice, S. a. and Mackerras, D. (1977) ‘The Ratio of Cloud to Cloud-Ground Lightning Flashes in Thunderstorms’, *Journal of Applied Meteorology*, pp. 545–550. doi: 10.1175/1520-0450(1977)016<0545:TROCTC>2.0.CO;2.

Randerson, J. T., Liu, H., Flanner, M. G., Chambers, S. D., Jin, Y., Hess, P. G., Pfister, G., Mack, M. C., Treseder, K. K., Welp, L. R., Chapin, F. S., Harden, J. W., Goulden, M. L., Lyons, E., Neff, J. C., Schuur, E. a G. and Zender, C. S. (2006) ‘The impact of boreal forest fire on climate warming.’, *Science*, 314(5802), pp. 1130–1132. doi: 10.1126/science.1132075.

Randerson, J. T., Chen, Y., Van Der Werf, G. R., Rogers, B. M. and Morton, D. C. (2012) ‘Global burned area and biomass burning emissions from small fires’, *Journal of Geophysical Research: Biogeosciences*, 117(4). doi: 10.1029/2012JG002128.

Rogers, B. M., Soja, A. J., Goulden, M. L. and Randerson, J. T. (2015) ‘Influence of tree species on continental differences in boreal fires and climate feedbacks’, *Nature Geoscience*, 8(February), pp. 228–234. doi: 10.1016/j.cognition.2008.05.007.

Romps, D. M., Seeley, J. T., Vollaro, D. and Molinari, J. (2014) ‘Projected increase in lightning strikes in the United States due to global warming’, *Science*, 346(621), pp. 851–853. doi: 10.1126/science.1259100.

Sankaran, M., Ratnam, J. and Hanan, N. P. (2004) ‘Tree-grass coexistence in savannas revisited - Insights from an examination of assumptions and mechanisms invoked in existing models’, *Ecology Letters*, 7(6), pp. 480–490. doi: 10.1111/j.1461-0248.2004.00596.x.

Schneider, U., Becker, A., Finger, P., Meyer-Christoffer, A., Ziese, M. and Rudolf, B. (2014) ‘GPCC’s new land surface precipitation climatology based on quality-controlled in situ data and its role in quantifying the global water cycle’, *Theoretical and Applied Climatology*, 115(1–2), pp. 15–40. doi: 10.1007/s00704-013-0860-x.

Stahl, C., Hérault, B., Rossi, V., Burban, B., Bréchet, C. and Bonal, D. (2013) ‘Depth of soil water uptake by tropical rainforest trees during dry periods: does tree dimension matter?’, *Oecologia*, 173(4), pp. 1191–1201. doi: 10.1007/s00442-013-2724-6.

Syphard, A. D., Radeloff, V. C., Hawbaker, T. J. and Stewart, S. I. (2009) ‘Conservation threats due to human-caused increases in fire frequency in mediterranean-climate ecosystems’, *Conservation Biology*, 23(3), pp. 758–769. doi: 10.1111/j.1523-1739.2009.01223.x.

Tacconi, L. (2003) ‘Fires in Indonesia: causes, costs and policy implications’, *Centre for International Forestry Research (CIFOR) - CIFOR Infobrief*, (5), pp. 1–4.

Thonicke, K., Spessa, A., Prentice, I. C., Harrison, S. P., Dong, L. and Carmona-Moreno, C. (2010) ‘The influence of vegetation, fire spread and fire behaviour on biomass burning and trace gas emissions: Results from a process-based model’, *Biogeosciences*, 7(6), pp. 1991–2011. doi: 10.5194/bg-7-1991-2010.

Thonicke, K., Venevsky, S., Sitch, S. and Cramer, W. (2001) ‘The role of fire disturbance for global vegetation dynamics: coupling fire into a Dynamic Global Vegetation Model’, *Global Ecology and Biogeography*, 10(6), pp. 661–677. doi: 10.1046/j.1466-822X.2001.00175.x.

Tosca, M. G., Randerson, J. T. and Zender, C. S. (2013) ‘Global impact of smoke aerosols from landscape fires on climate and the Hadley circulation’, *Atmospheric Chemistry and Physics*, 13(10), pp. 5227–5241. doi: 10.5194/acp-13-5227-2013.

Venevsky, S., Thonicke, K., Sitch, S. and Cramer, W. (2002) ‘Simulating fire regimes in human-dominated ecosystems: Iberian Peninsula case study’, *Global Change Biology*, 8(10), pp. 984–998. doi: 10.1046/j.1365-2486.2002.00528.x.

Ward, D. S., Kloster, S., Mahowald, N. M., Rogers, B. M., Randerson, J. T. and Hess, P. G. (2012) ‘The changing radiative forcing of fires: global model estimates for past, present and future’, *Atmospheric Chemistry and Physics*, 12(22), pp. 10857–10886. doi: 10.5194/acp-12-10857-2012.

van der Werf, G. R. (2004) ‘Continental-Scale Partitioning of Fire Emissions During the 1997 to 2001 El Nino/La Nina Period’, *Science*. American Association for the Advancement of Science, 303(5654), pp. 73–76. doi: 10.1126/science.1090753.

van der Werf, G. R., Randerson, J. T., Giglio, L., Collatz, G. J., Kasibhatla, P. S. and Arellano, Avelino F., J. (2006) ‘Interannual variability in global biomass burning emissions from 1997 to 2004’, *Atmospheric Chemistry and Physics*, 6(11), pp. 3423–3441. doi: 10.5194/acpd-6-3175-2006.

Van Der Werf, G. R., Randerson, J. T., Giglio, L., Collatz, G. J., Mu, M., Kasibhatla, P. S., Morton, D. C., Defries, R. S., Jin, Y. and Van Leeuwen, T. T. (2010) ‘Global fire emissions and the contribution of deforestation, savanna, forest, agricultural, and peat fires (1997-2009)’, *Atmospheric Chemistry and Physics*, 10(23), pp. 11707–11735. doi: 10.5194/acp-10-11707-2010.

Werner, P. A. (2005) ‘Impact of feral water buffalo and fire on growth and survival of mature savanna trees: An experimental field study in Kakadu National Park, northern Australia’, *Austral Ecology*, 30(6), pp. 625–647. doi: 10.1111/j.1442-9993.2005.01491.x.

Westerling, A. L., Hidalgo, H. G., Cayan, D. R. and Swetnam, T. W. (2006) ‘Warming and earlier spring increase western U.S. forest wildfire activity’, *Science*, 313(5789), pp. 940–3. doi: 10.1126/science.1128834.

Williams, R. J., Bradstock, R. A., Cary, G. J., Enright, N. J., Gill, A. M., Liedloff, A. C., Lucas, C., Whelan, R. J., Andersen, A. N., Bowman, D. J., CLarke, P. J., Cook, G. D., Hennessy, K. J. and York, A. (2009) ‘Interactions between climate change, fire regimes and biodiversity in Australia: a preliminary assessment’, *Department of Climate Change, Canberra*, 17, p. 196.

Yang, J., Tian, H., Tao, B., Ren, W., Lu, C., Pan, S., Wang, Y. and Liu, Y. (2015) ‘Century-scale patterns and trends of global pyrogenic carbon emissions and fire influences on terrestrial carbon balance’, *Global Biogeochemical Cycles*, 29(9), pp. 1549–1566. doi: 10.1002/2015GB005160.

Yue, C., Ciais, P., Cadule, P., Thonicke, K., Archibald, S., Poulter, B., Hao, W. M., Hantson, S., Mouillot, F., Friedlingstein, P., Maignan, F. and Viovy, N. (2014) ‘Modelling the role of fires in the terrestrial carbon balance by incorporating SPITFIRE into the global vegetation model ORCHIDEE – Part 1: simulating historical global burned area and fire regimes’, *Geoscientific Model Development*, 7(6), pp. 2747–2767. doi: 10.5194/gmd-7-2747-2014.

Annex A – Figures

Figure A1:Relative humidity simulated with or without prescribed standard deviation and observed, for the middle month of each season. Relative humidity over oceans was kept by mistake for the observed data as for simulated data.

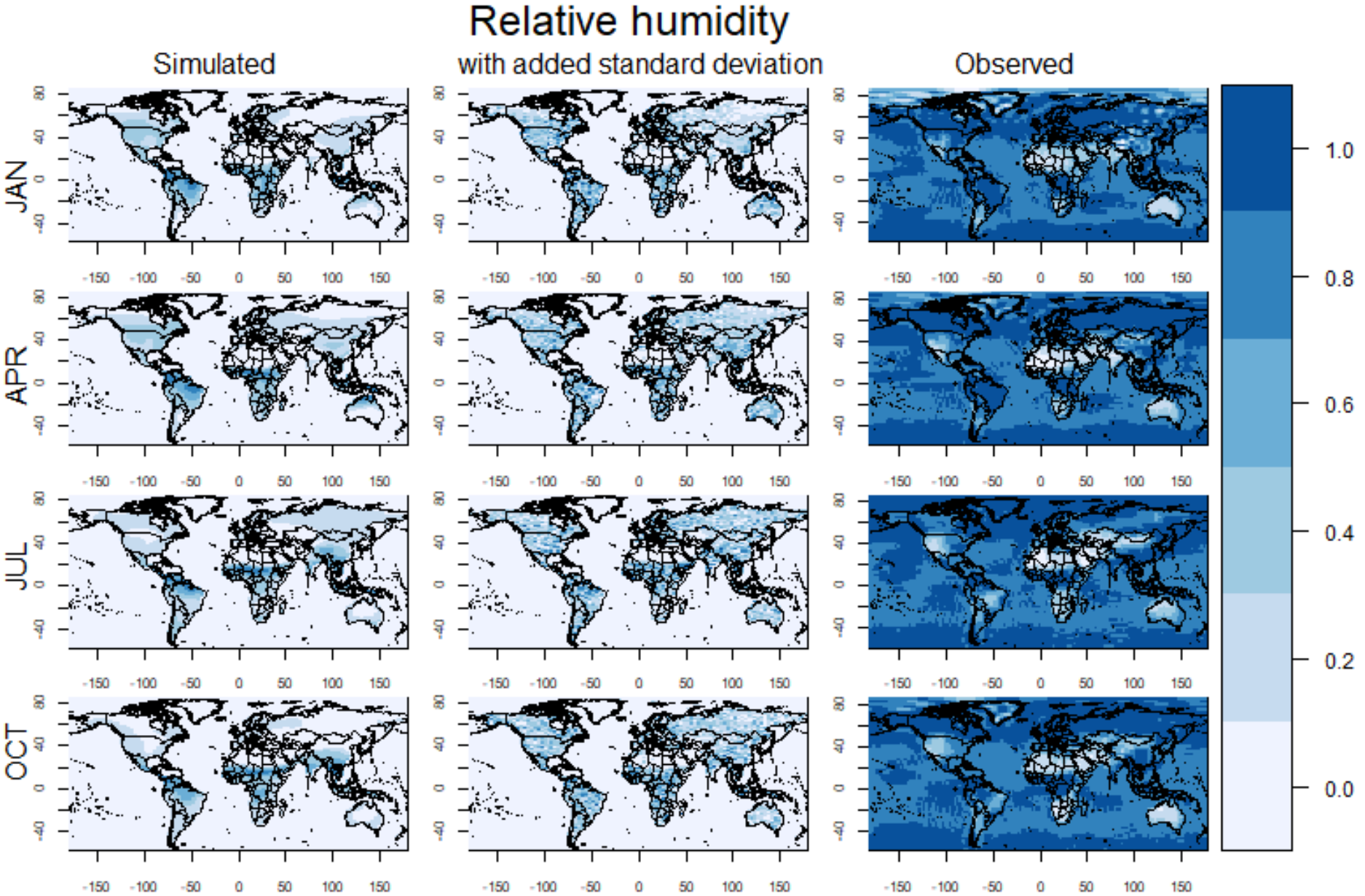

Figure A2:Soil moisture simulated with or without prescribed standard deviation and observed, for the middle month of each season.

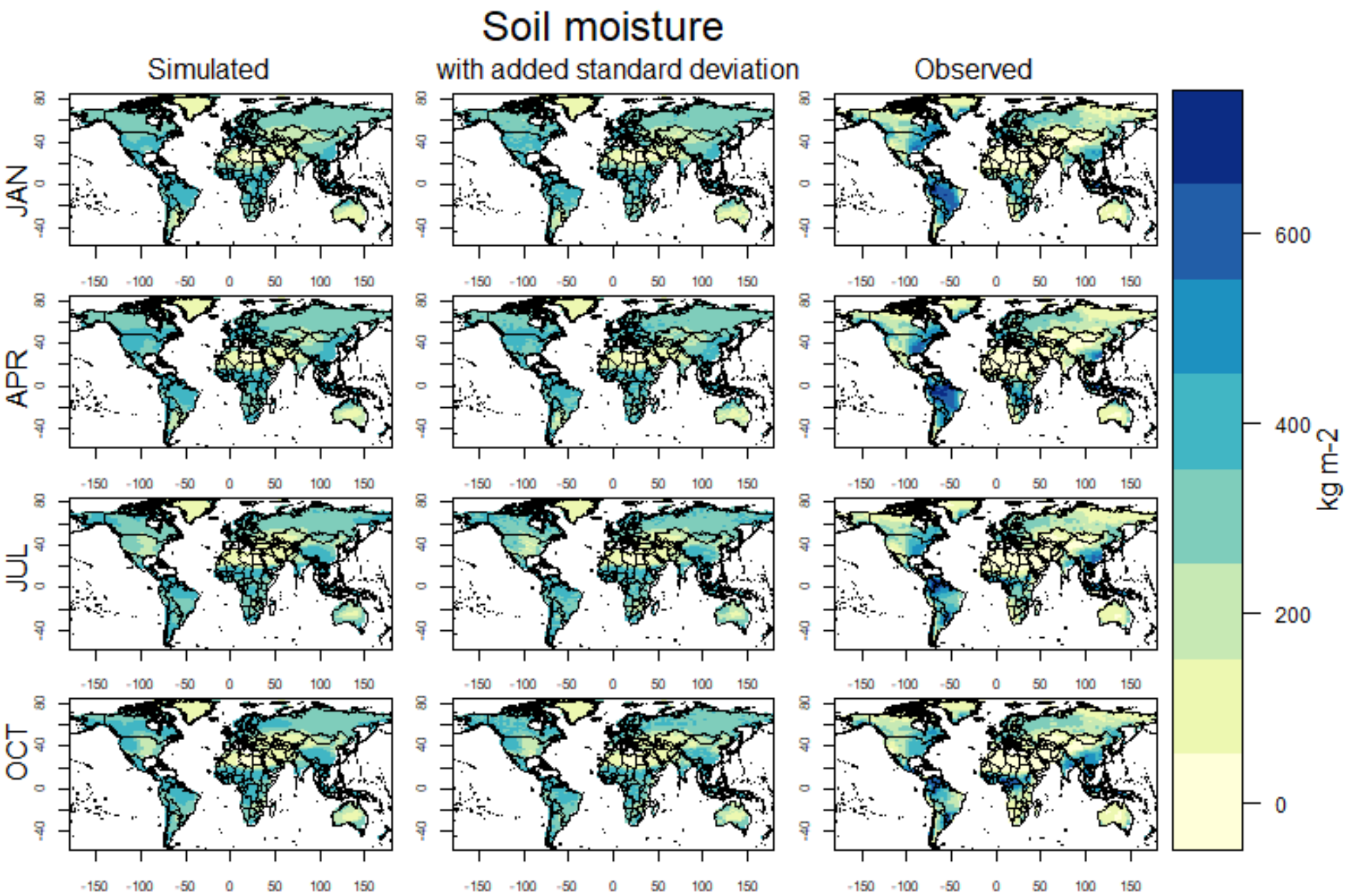

Figure A3: The model settings are given in table 3. The correlation coefficient R was calculated relative to the GFED4 dataset.

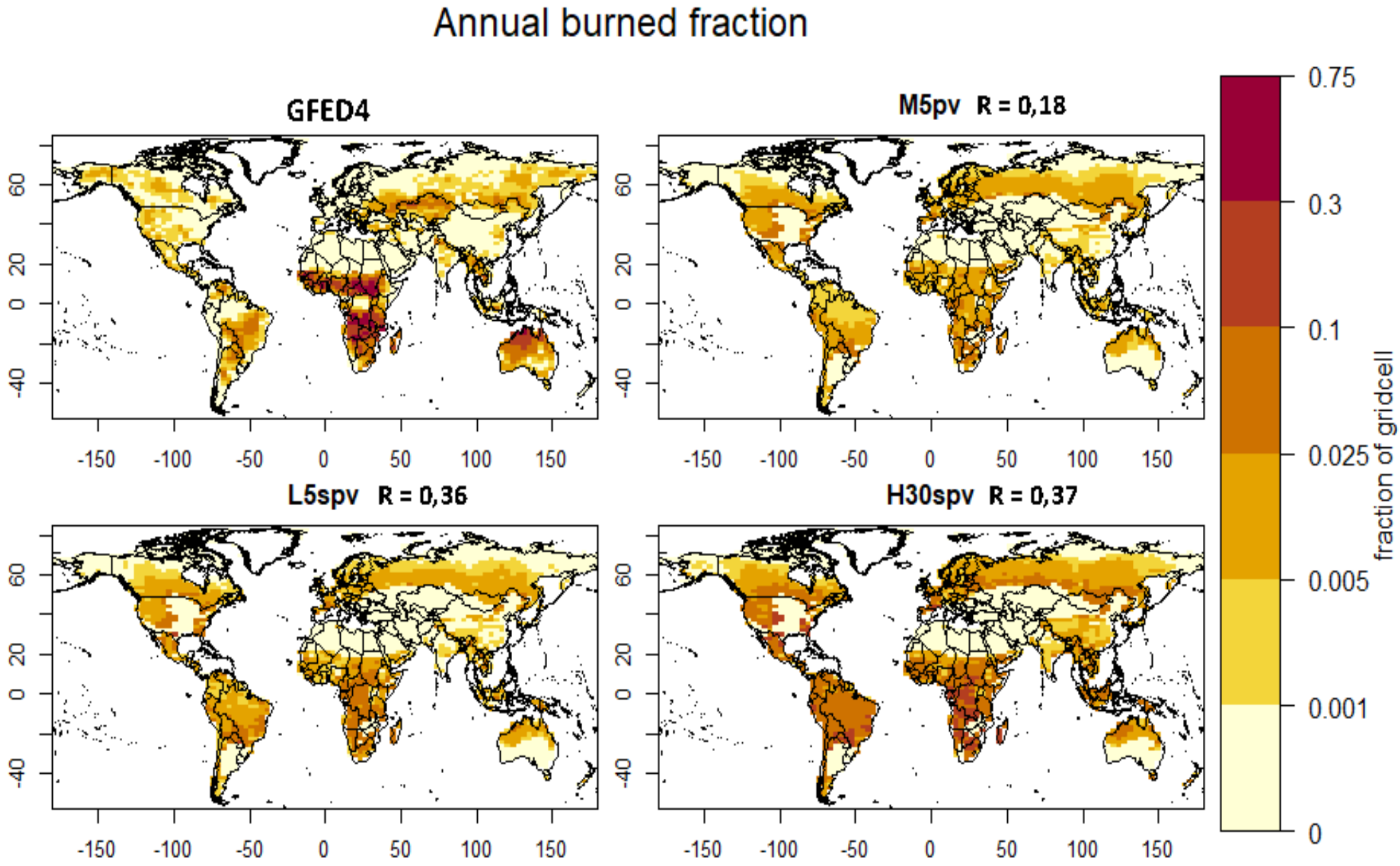

Figure A4: The model settings are given in table 3. The correlation coefficient R was calculated relative to the GFED4 dataset.

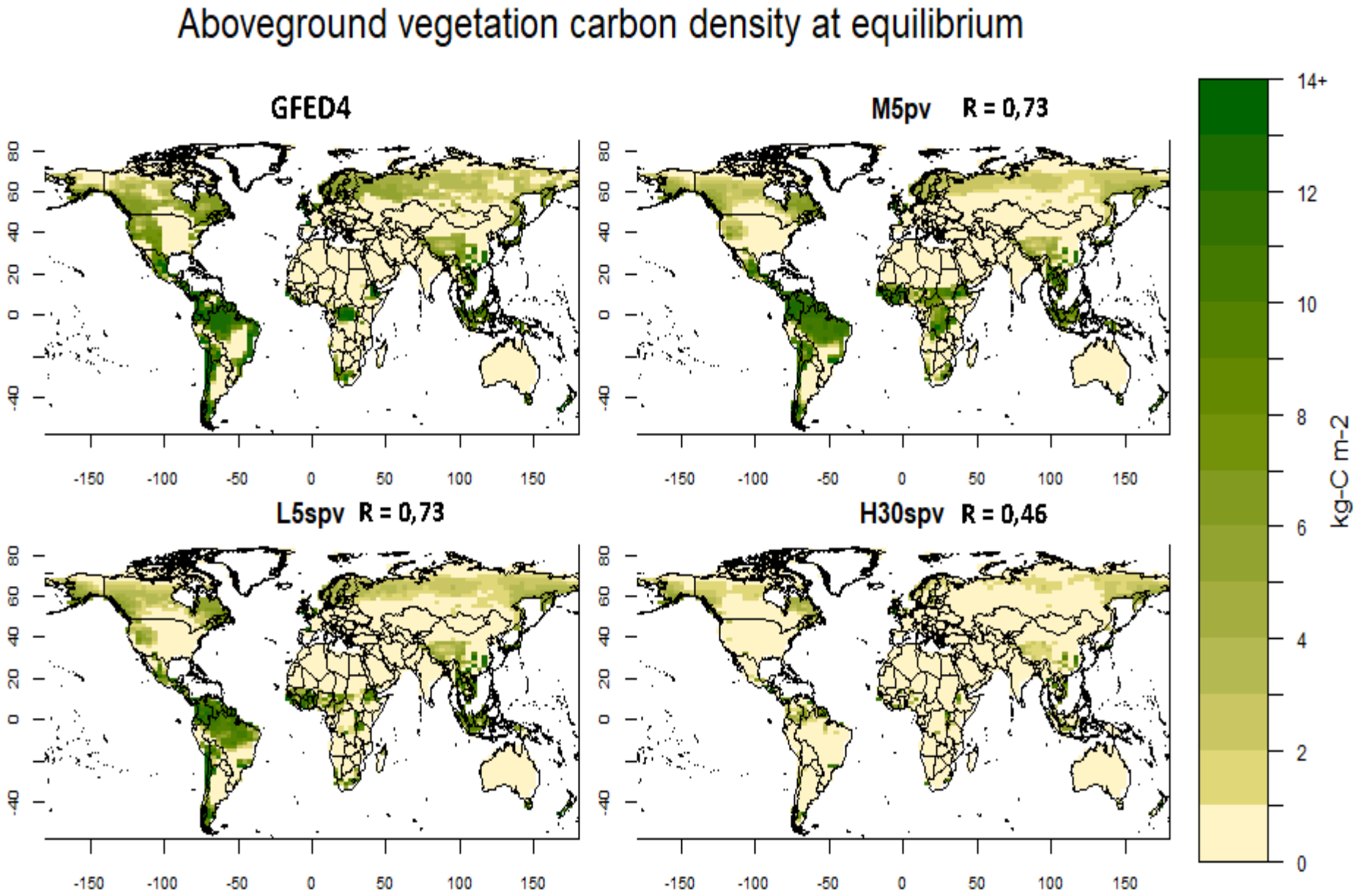

Figure A5: Observed above- and below-ground vegetation carbon. The units (t – C/ha) divided by 10 match the ones from Figure A6. Figure taken from Ruesch & Gibbs (2008).

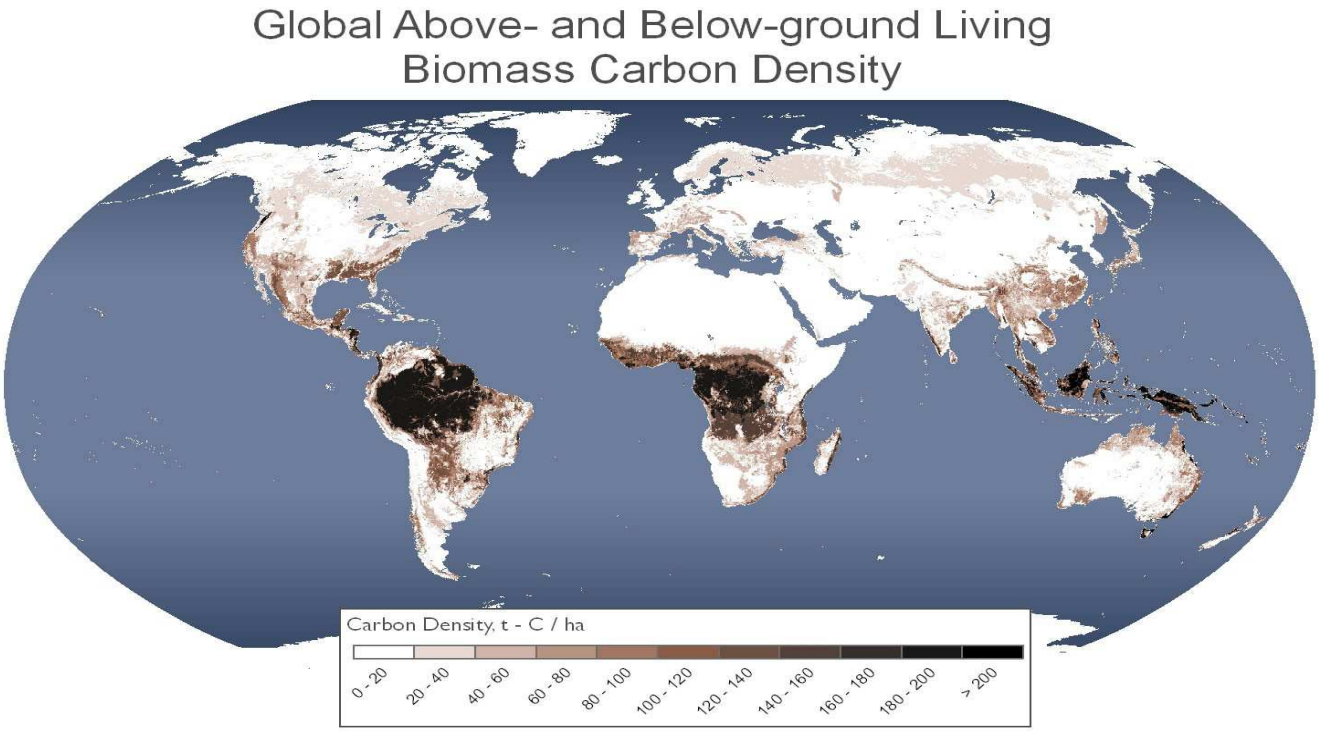

Figure A6: Simulated aboveground vegetation carbon at equilibrium without fire. The units (kg-C m^{-2}) multiplied by 10 match the ones from Figure A5.

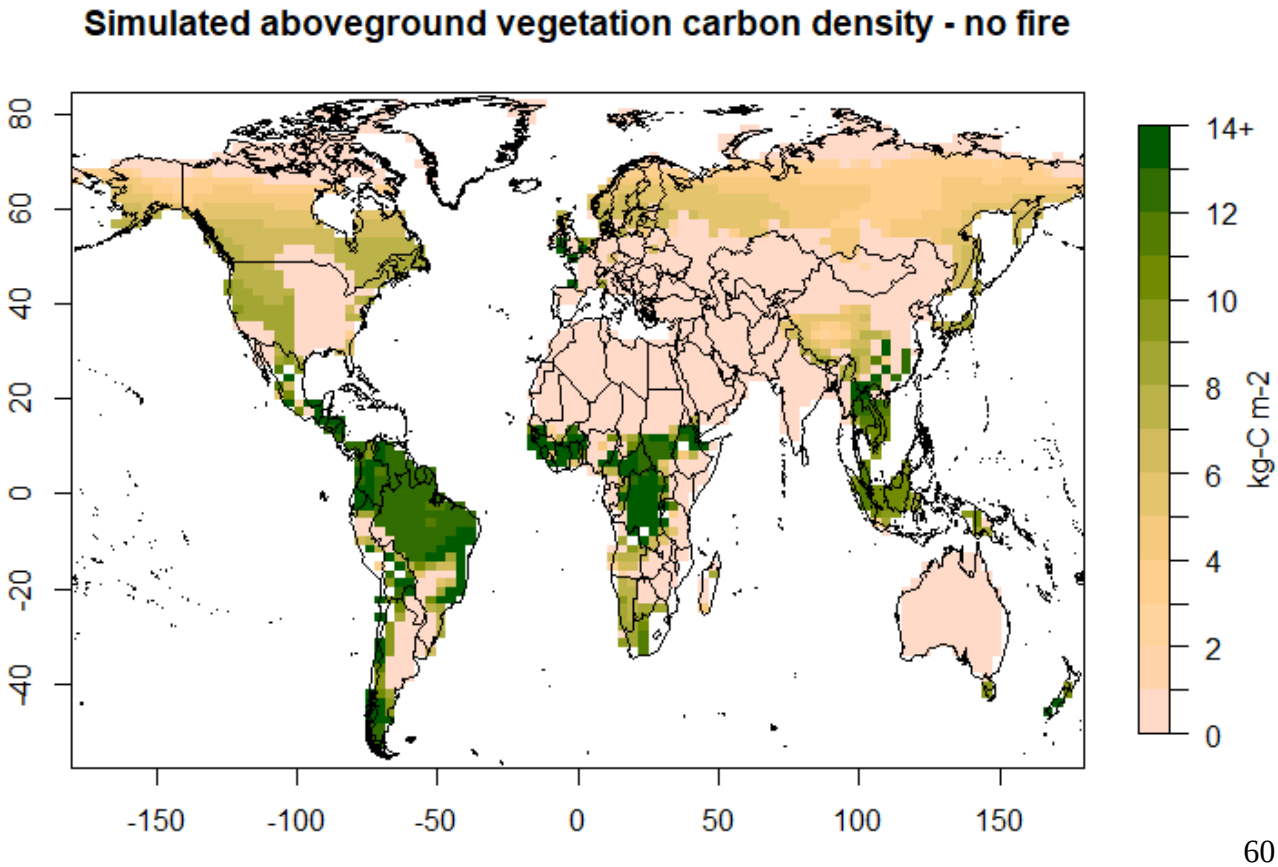

Figure A7: Annual fire counts observed by MODIS (Giglio et al. 2006). Figure taken from Bowman et al. (2009)

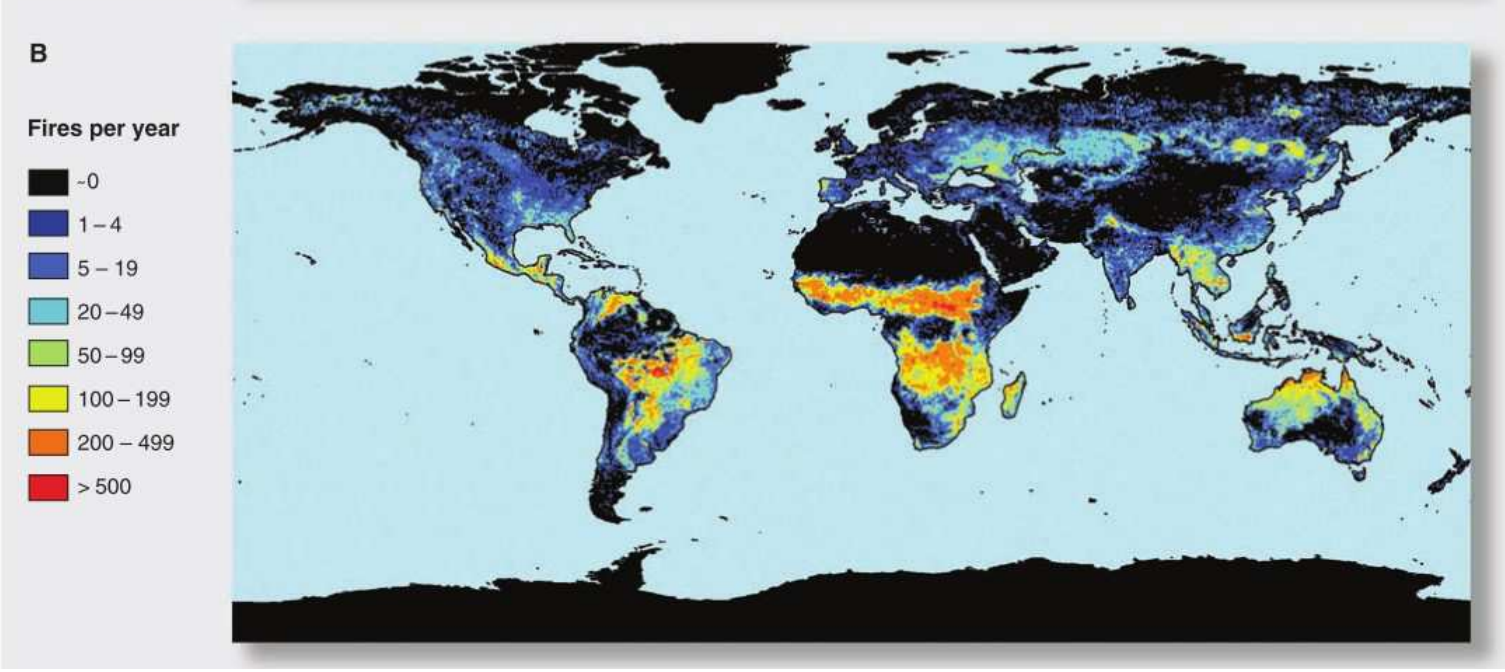

Figure A8: Annual fire counts simulated by the L5spv simulation (see table 3 for model description). Firecounts per gridcell were adjusted to match the units of Figure A7.

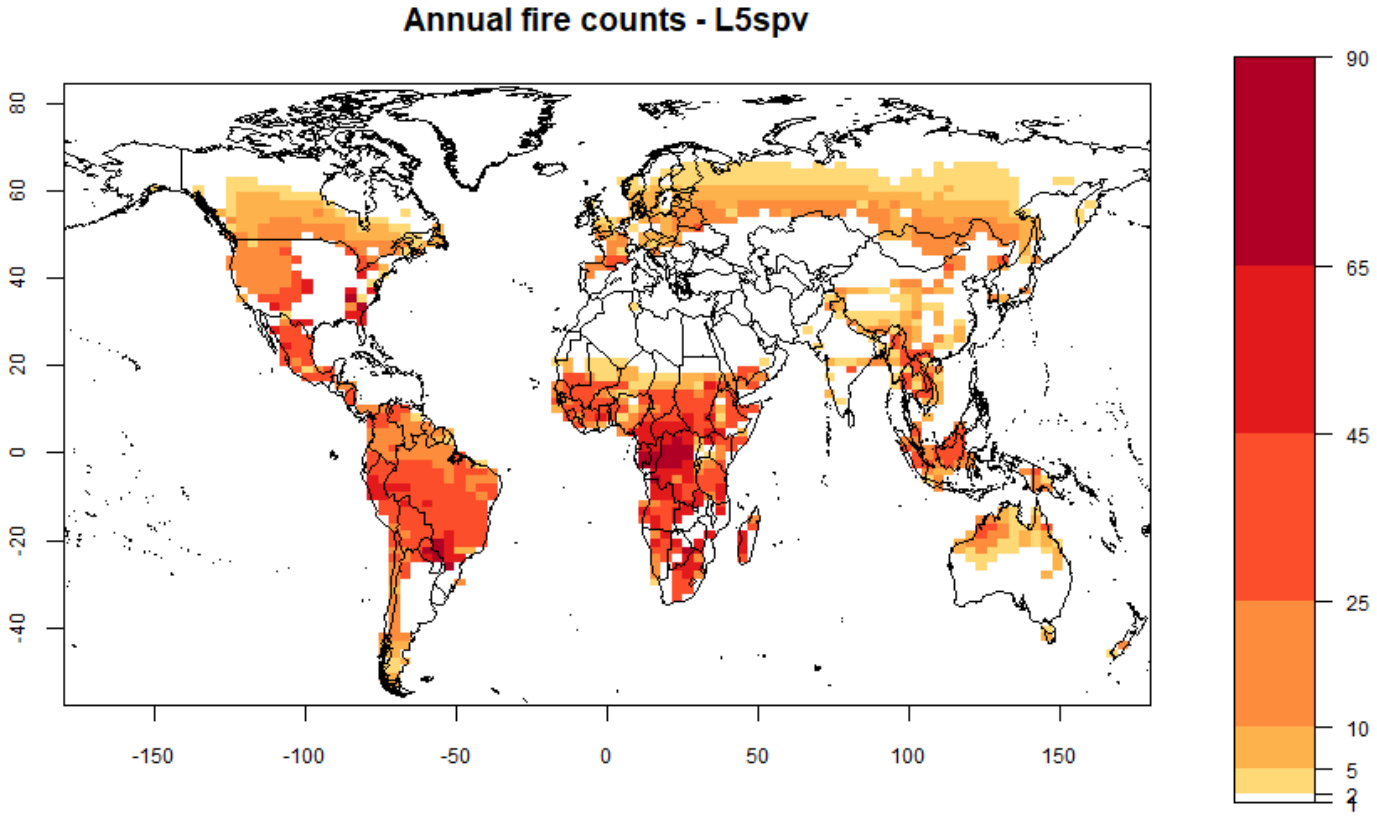

Figure A9: Annual flash count prescribed to the fire parameterization based on 1995-2013. See Table 2 for source.